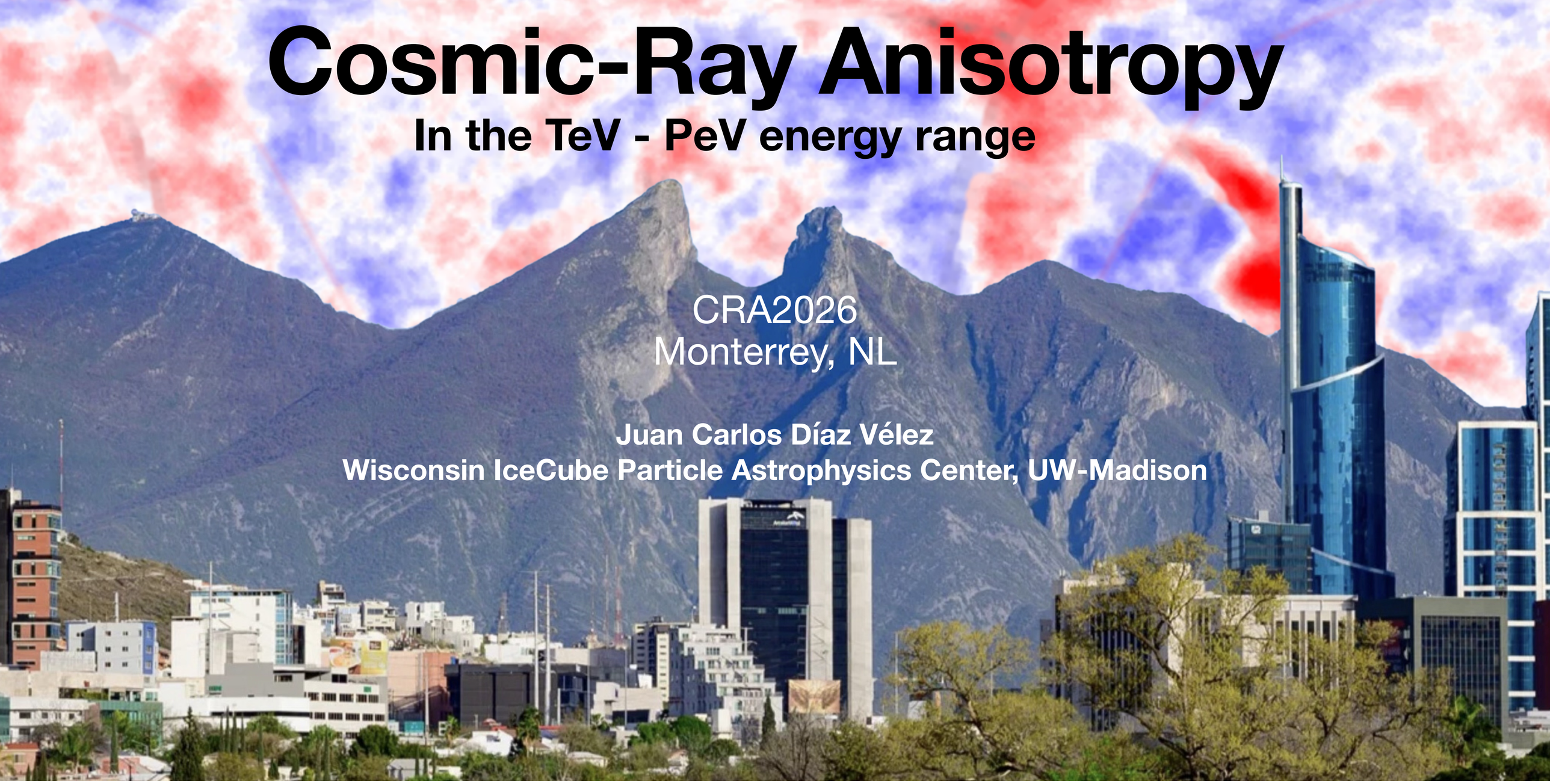
Cosmic-Ray Anisotropy

In the TeV - PeV energy range



CRA2026
Monterrey, NL

Juan Carlos Díaz Vélez
Wisconsin IceCube Particle Astrophysics Center, UW-Madison

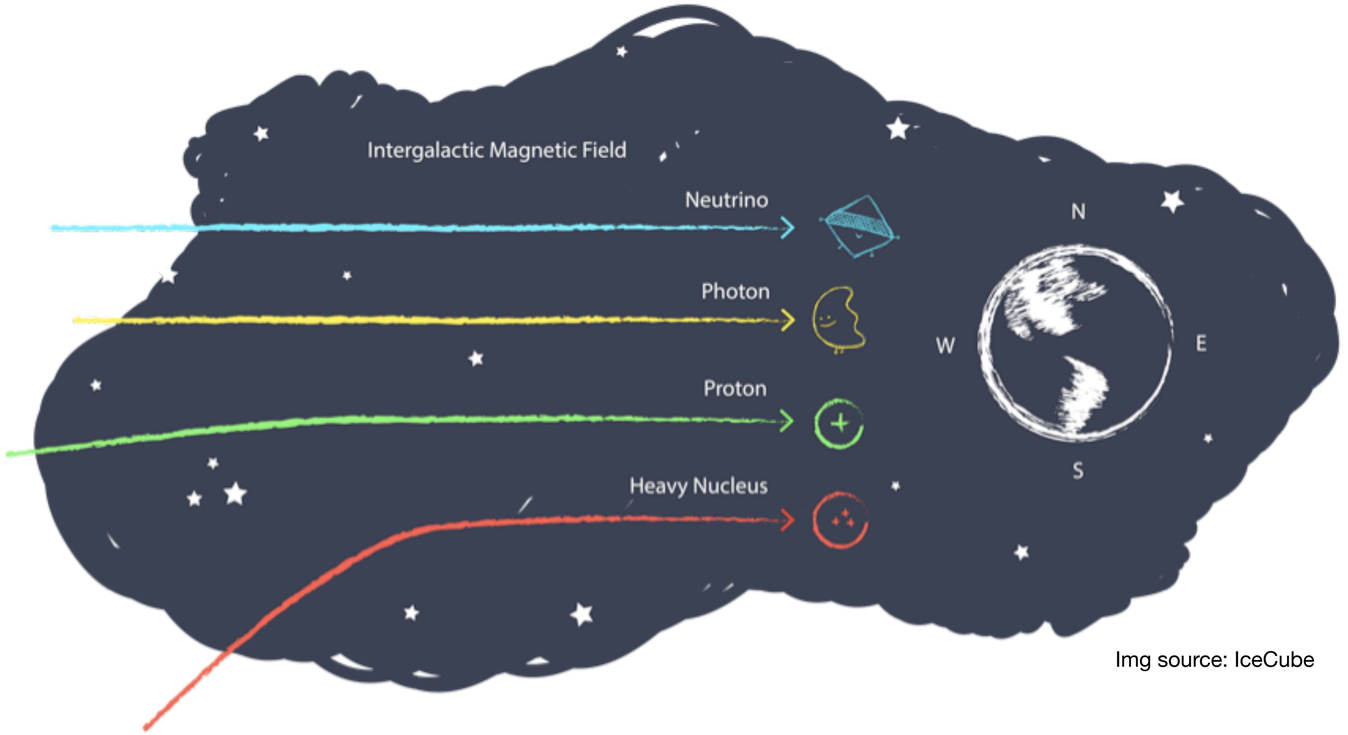
Propagation of particles in magnetic fields

Cosmic rays are deflected by interstellar magnetic fields and become diffusive through pitch angle scattering and mirror diffusion in the turbulent interstellar medium.

Their arrival directions are determined by the distribution of galactic sources and by their propagation through the turbulent and inhomogeneous interstellar magnetized plasma.

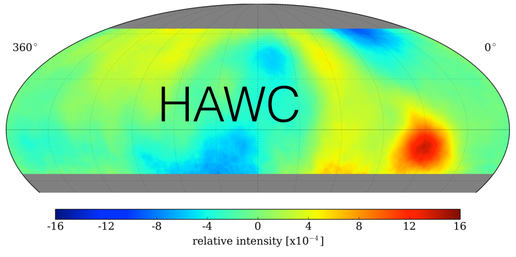
After traveling long distances through the Galaxy, we would expect the arrival direction distribution to be completely randomized.

However, ...

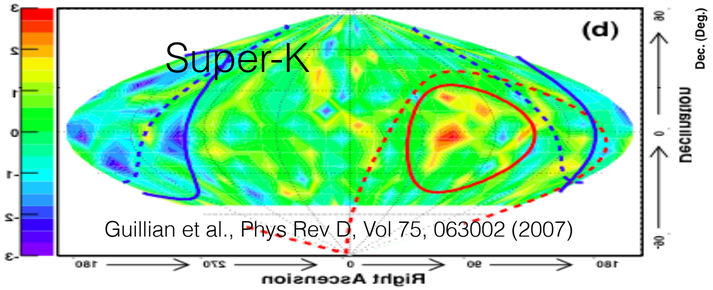


Img source: IceCube

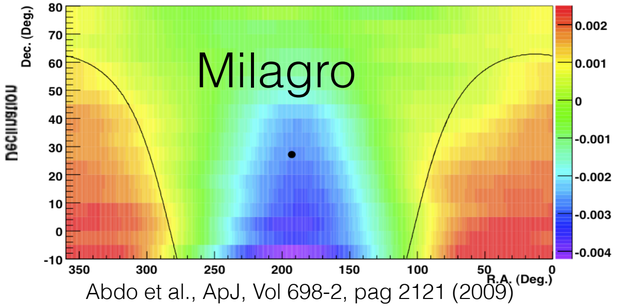
Over the last few decades, several studies have measured a large scale anisotropy at a level of10^{-3} and a small-scale structure with an amplitude of 10^{-4} and angular size from 10° to 30°.



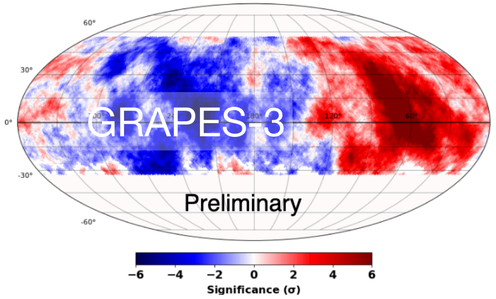
A. U. Abeysekara et al. Astrophys. J. (2014)

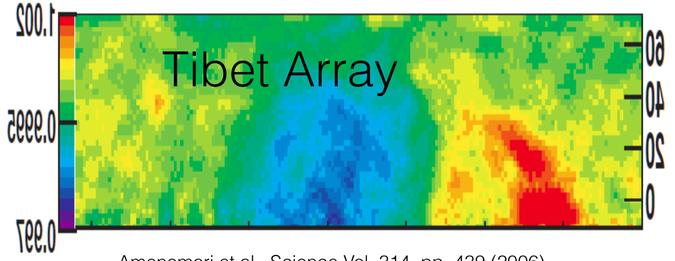


Guillian et al., Phys Rev D, Vol 75, 063002 (2007)

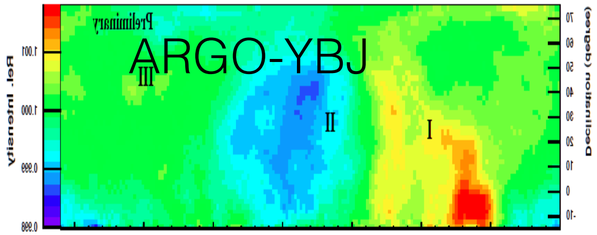


Abdo et al., ApJ, Vol 698-2, pag 2121 (2009)





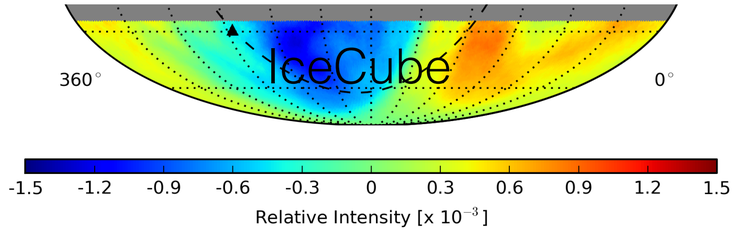
Amenomori et al., Science Vol. 314, pp. 439 (2006)



Zhang et al. Proc. 32nd ICRC (2009)

North

South

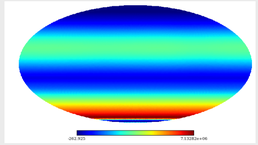


M. G. Aartsen et al. Astrophys.J. 826 (2016)

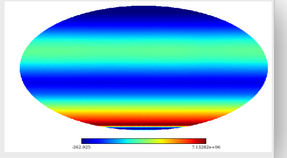
Large-scale features in South appear to be a continuation of those observed in the Northern Hemisphere.

Method for measuring CR anisotropy

1 Build a binned data map using the equatorial coordinates of the events



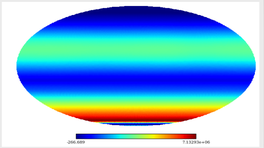
2 Construct a “reference” map by integrating acceptance over 24 hours.



Time-scrambling:

$$(\theta, \phi, t) \rightarrow (\alpha, \delta)$$
$$(\theta, \phi, t') \rightarrow (\alpha', \delta')$$

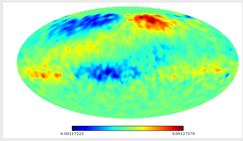
3 Correlate pixels to increase sensitivity to different angular scales



Relative Intensity

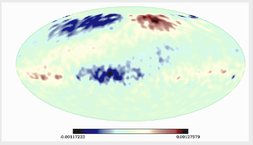
$$\delta I(\alpha,\delta)_i = \frac{N(\alpha,\delta)_i - \langle N\rangle(\alpha,\delta)_i}{\langle N\rangle(\alpha,\delta)_i}$$

4 Calculate relative differences between data and reference with significance.



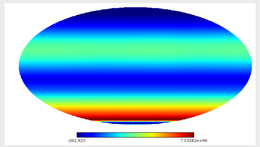
$$s_i = \sqrt{2}\left\{N_i \log\left[\frac{1+\alpha}{\alpha}\left(\frac{N_i}{N_i+N_o}\right)\right] + N_o \log\left[(1+\alpha)\left(\frac{N_o}{N_i+N_o}\right)\right]\right\}^{1/2}$$

5 Calculate statistical significance for each pixel

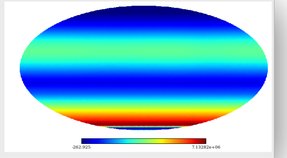


Method for measuring CR anisotropy

1 Build a binned data map using the equatorial coordinates of the events



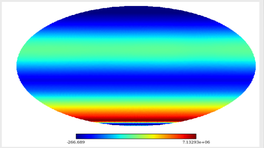
2 Construct a “reference” map by integrating acceptance over 24 hours.



Maximum LLH method (M. Ahlers, et al. 2016):

$$\mathcal{L}(n|I,\mathcal{N},\mathcal{A}) = \prod_{\tau i} \frac{(\mu_{\tau i})^{n_{\tau i}} e^{-\mu_{\tau i}}}{n_{\tau i}!}$$

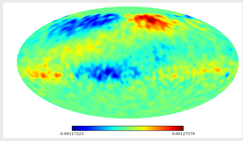
3 Correlate pixels to increase sensitivity to different angular scales



Relative Intensity

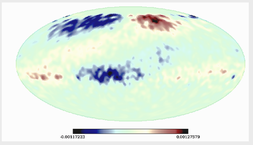
$$\delta I(\alpha,\delta)_i = \frac{N(\alpha,\delta)_i - \langle N\rangle(\alpha,\delta)_i}{\langle N\rangle(\alpha,\delta)_i}$$

4 Calculate relative differences between data and reference with significance.



$$s_i = \sqrt{2}\left\{ N_i \log\left[\frac{1+\alpha}{\alpha}\left(\frac{N_i}{N_i+N_o}\right)\right] + N_o \log\left[(1+\alpha)\left(\frac{N_o}{N_i+N_o}\right)\right]\right\}^{1/2}$$

5 Calculate statistical significance for each pixel



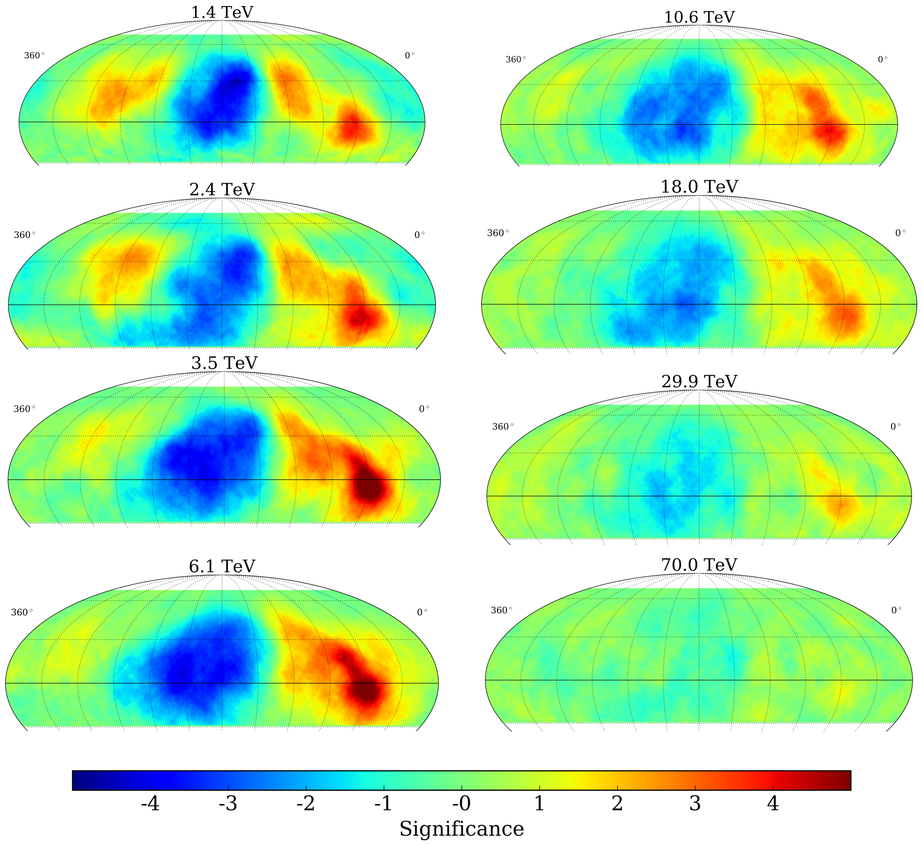
Anisotropy Measurements as a Function of Energy

The Astrophysical Journal, 865:57 (15pp), 2018 September 20 https://doi.org/10.3847/1538-4357/aad90c
© 2018. The American Astronomical Society. All rights reserved.

Observation of Anisotropy of TeV Cosmic Rays with Two Years of HAWC

A. U. Abeysekara[1], R. Alfaro[2], C. Alvarez[3], J. D. Álvarez[4], R. Arceo[3], J. C. Arteaga-Velázquez[4], D. Avila Rojas[2],

HAWC

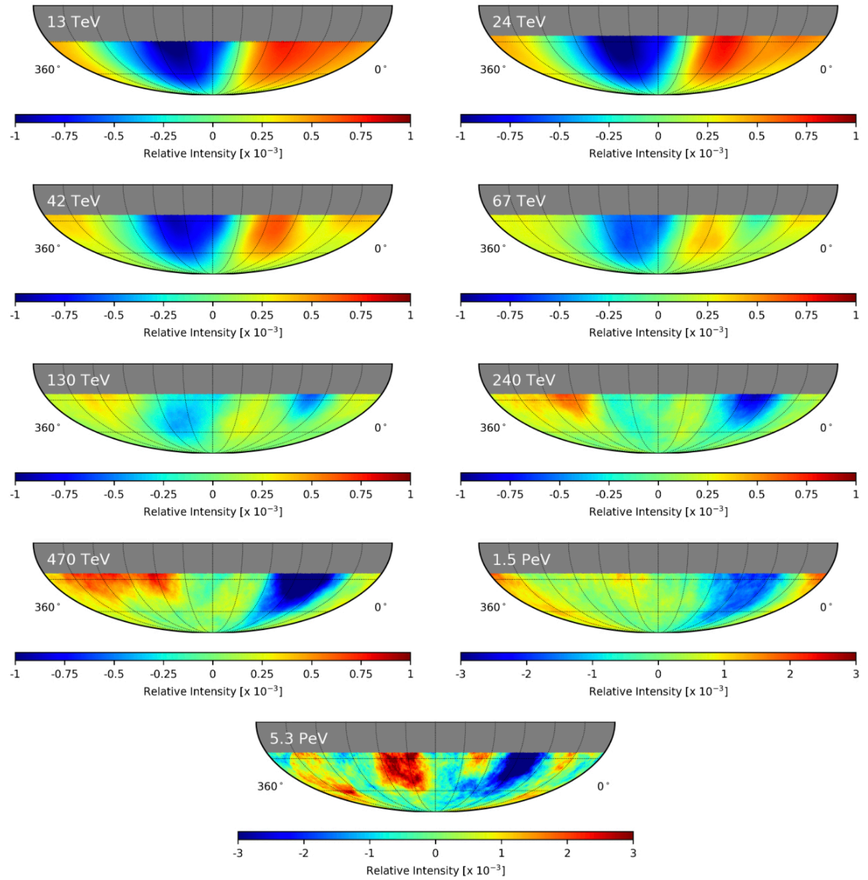


The Astrophysical Journal, 981:182 (20pp), 2025 March 10 https://doi.org/10.3847/1538-4357/adb1de
© 2025. The Author(s). Published by the American Astronomical Society.
OPEN ACCESS

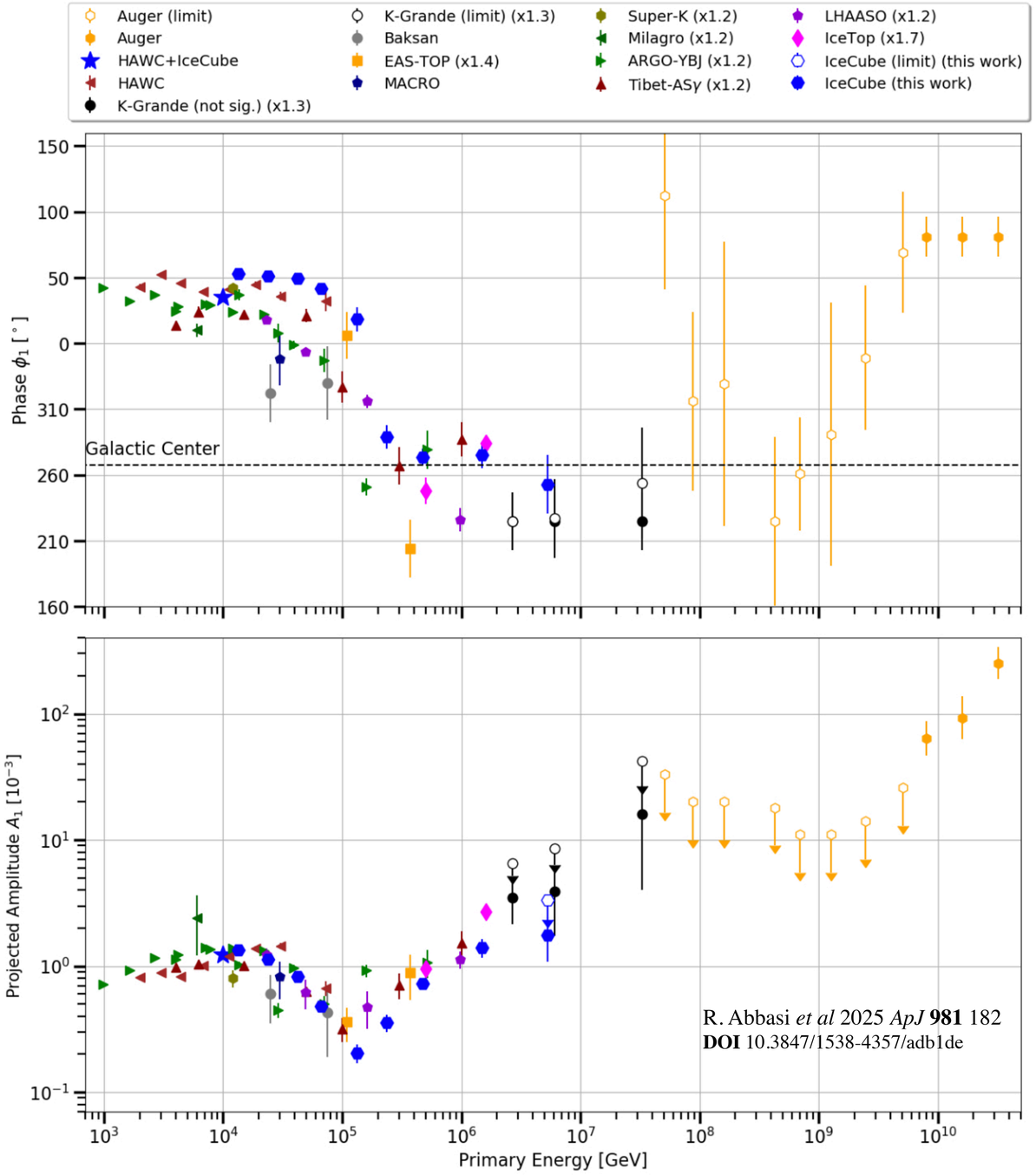
Observation of Cosmic-Ray Anisotropy in the Southern Hemisphere with 12 yr of Data Collected by the IceCube Neutrino Observatory

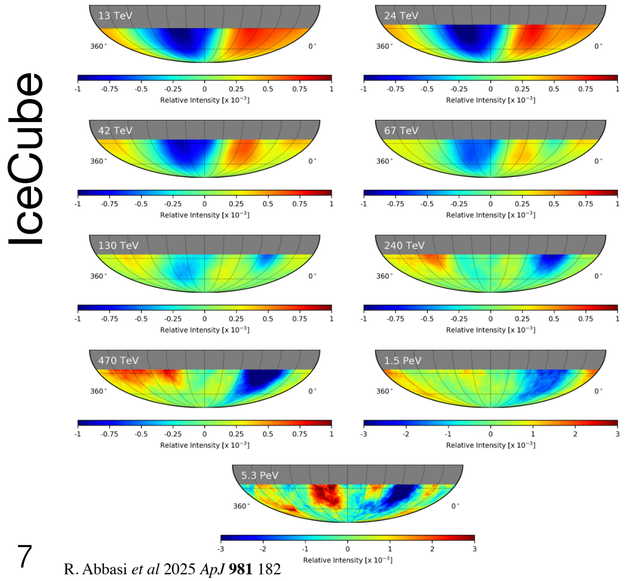
R. Abbasi[1], M. Ackermann[2], J. Adams[3], S. K. Agarwalla[4,66], T. Aguado[1], J. A. Aguilar[5], M. Ahlers[6],

IceCube

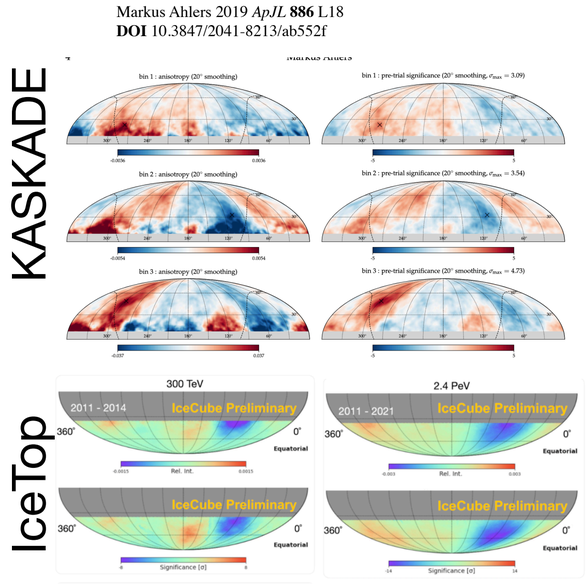


Dipole Component vs. Energy



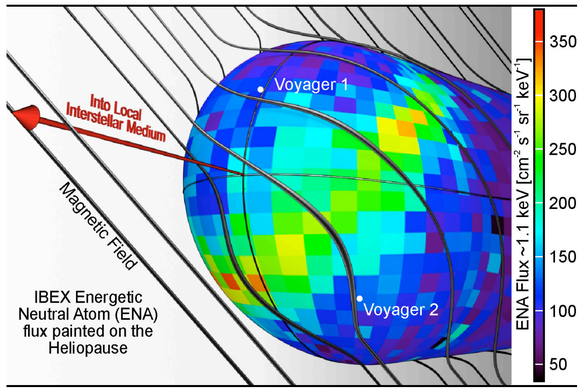


R. Abbasi *et al* 2025 *ApJ* **981** 182
DOI 10.3847/1538-4357/adb1de



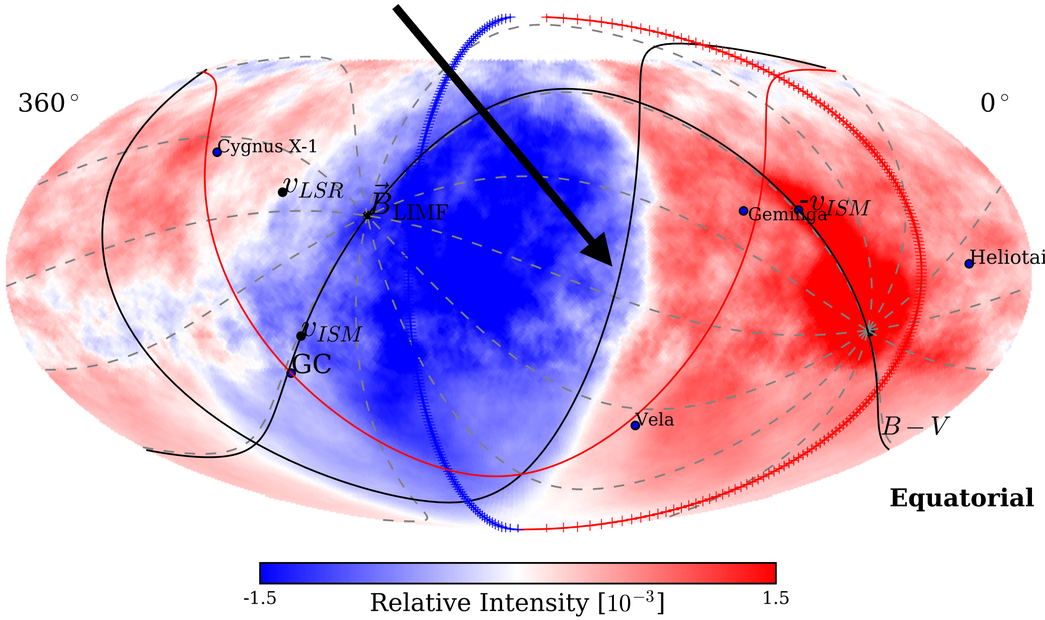
Markus Ahlers 2019 *ApJL* **886** L18
DOI 10.3847/2041-8213/ab552f

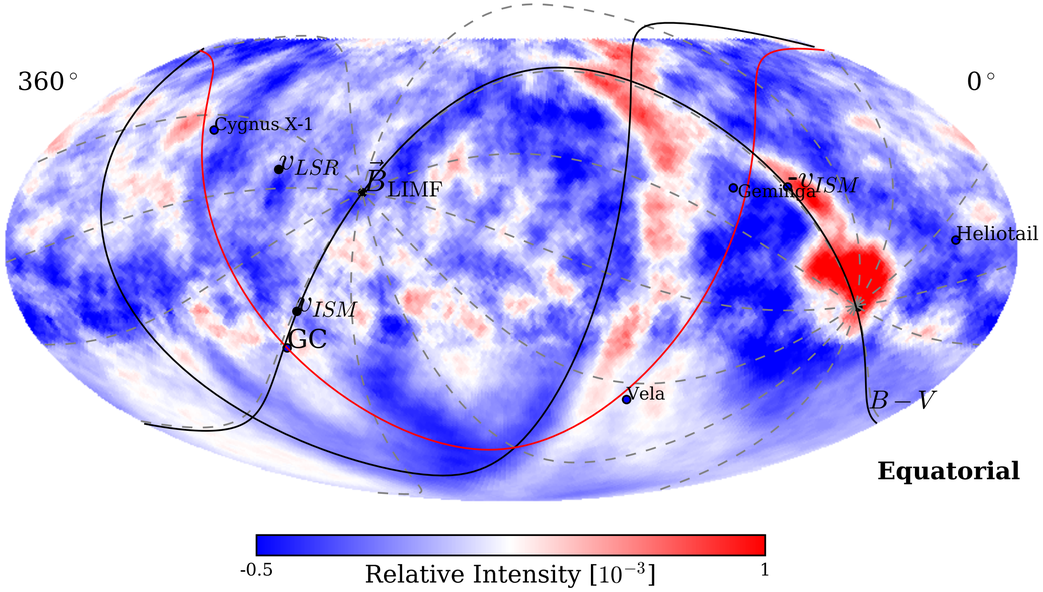
The Heliosphere and the LIMF



D. J. McComas *et al*., *Science***326**,959-962(2009).
DOI:10.1126/science.1180906

Steep gradient aligns with plane perpendicular to LIMF

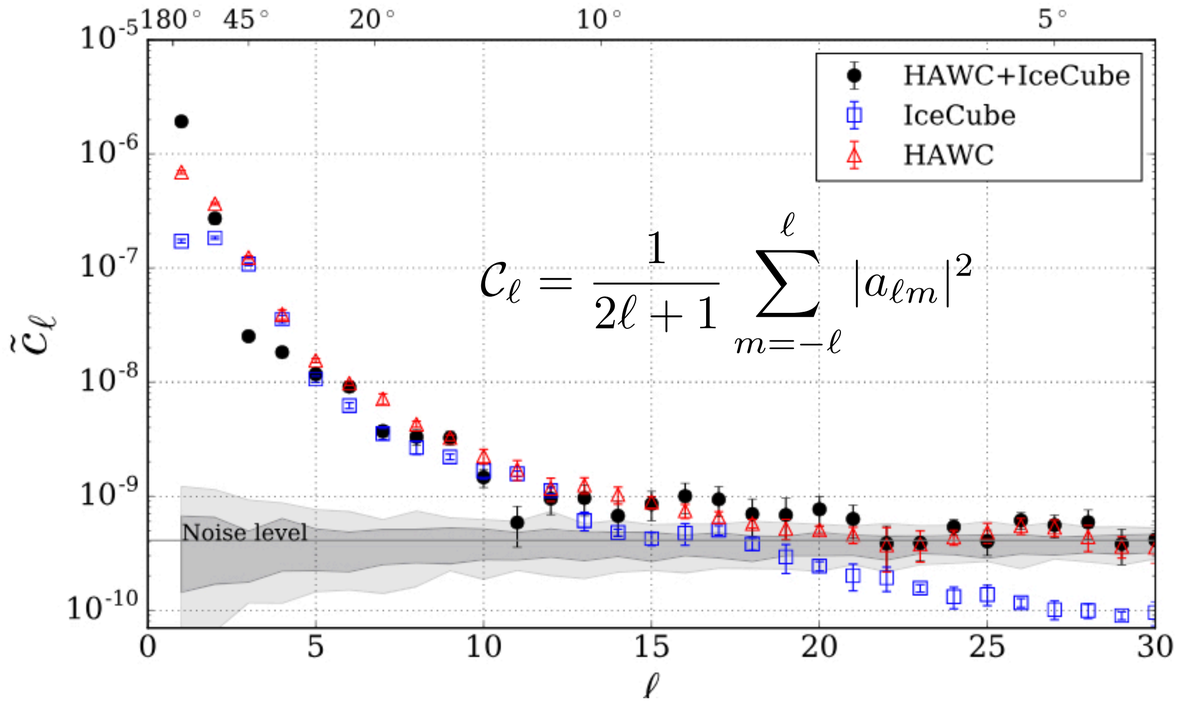




A. U. Abeysekara, et al. **DOI** 10.3847/1538-4357/aaf5cc

Angular Power Spectrum

M. Ahlers: Simple model of hierarchical structure of c_ℓ arising from the local turbulence of B-fields: higher multipole moments are induced locally by a global diffuse dipole moment within times Tv ≲ 1. Expect strength of individual multipoles to decreases in time.



A. U. Abeysekara, et al. **DOI** 10.3847/1538-4357/aaf5cc

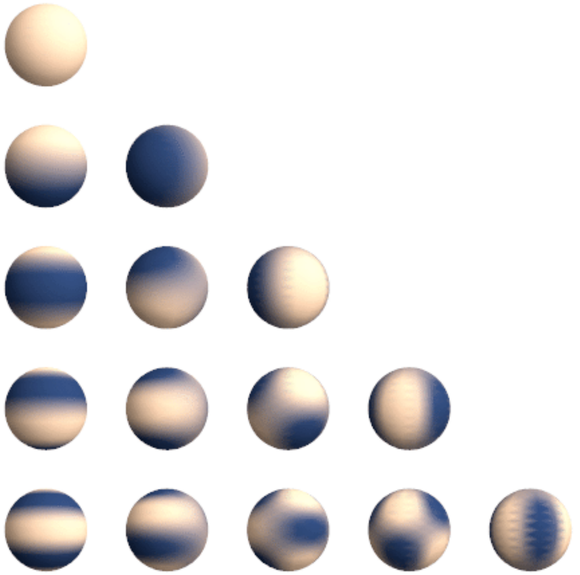
Spherical Harmonics

$$\delta I(\mathbf{u}_i) = \sum_{\ell=1}^{\infty} \sum_{m=-\ell}^{\ell} a_{\ell m} Y_{\ell m}(\mathbf{u}_i)$$

$$a_{\ell m} \sim \Omega_p \sum_{i=0}^{N_{\text{pix}}} \delta I(\mathbf{u}_i) Y^*_{\ell m}(\mathbf{u}_i).$$

$$Y_\ell^m(\theta, \varphi) = \sqrt{\frac{(2\ell+1)}{4\pi} \frac{(\ell-m)!}{(\ell+m)!}} P_\ell^m(\cos\theta)\, e^{im\varphi}$$

Legendre polynomials



Dipole

$$Y_1^{-1}(\theta, \varphi) = \frac{1}{2}\sqrt{\frac{3}{2\pi}}\, \sin\theta\, e^{-i\varphi}$$

$$Y_1^0(\theta, \varphi) = \frac{1}{2}\sqrt{\frac{3}{\pi}}\, \cos\theta$$

$$Y_1^1(\theta, \varphi) = \frac{-1}{2}\sqrt{\frac{3}{2\pi}}\, \sin\theta\, e^{i\varphi}$$

Quadrupole

$$Y_2^{-2}(\theta, \varphi) = \frac{1}{4}\sqrt{\frac{15}{2\pi}}\, \sin^2\theta\, e^{-2i\varphi}$$

$$Y_2^{-1}(\theta, \varphi) = \frac{1}{2}\sqrt{\frac{15}{2\pi}}\, \sin\theta\, \cos\theta\, e^{-i\varphi}$$

$$Y_2^0(\theta, \varphi) = \frac{1}{4}\sqrt{\frac{5}{\pi}}\, (3\cos^2\theta - 1)$$

$$Y_2^1(\theta, \varphi) = \frac{-1}{2}\sqrt{\frac{15}{2\pi}}\, \sin\theta\, \cos\theta\, e^{i\varphi}$$

$$Y_2^2(\theta, \varphi) = \frac{1}{4}\sqrt{\frac{15}{2\pi}}\, \sin^2\theta\, e^{2i\varphi}$$

https://en.wikipedia.org/wiki/Table_of_spherical_harmonics

Angular Power Spectrum

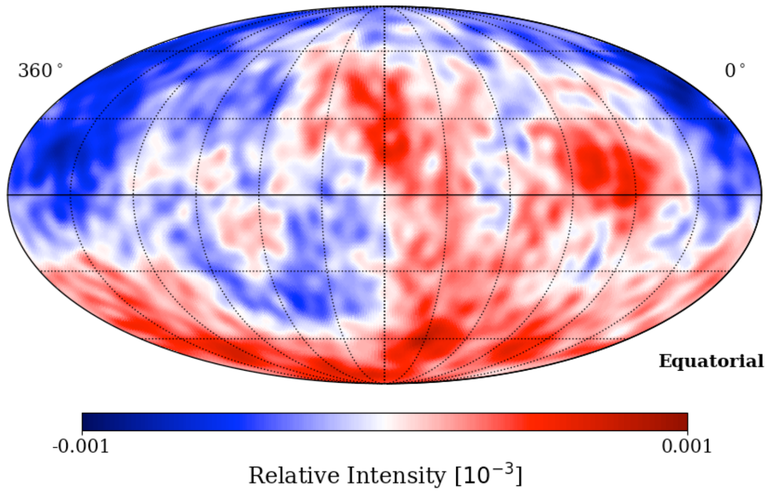
The APS provides an estimate of the significance of structures at different angular scales of

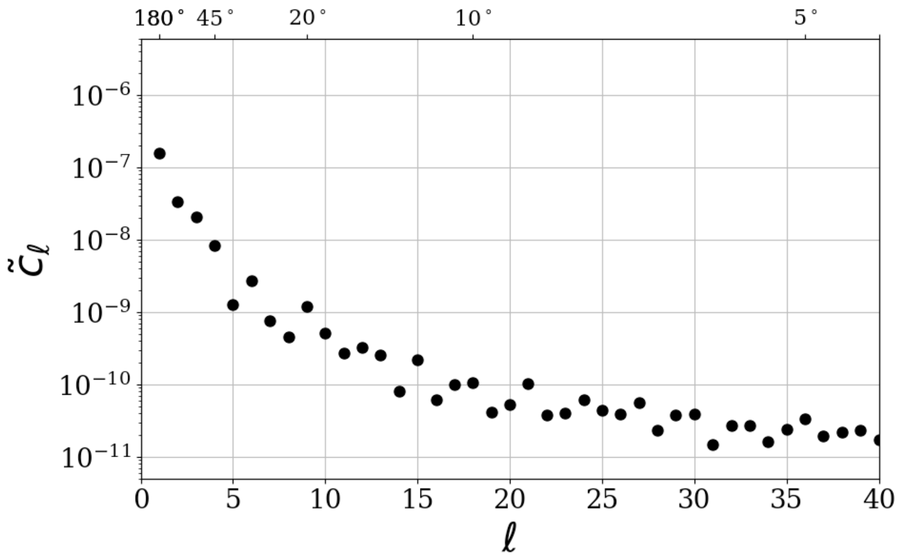
~ $180°/\ell$

We are completely blind to the m=0 terms

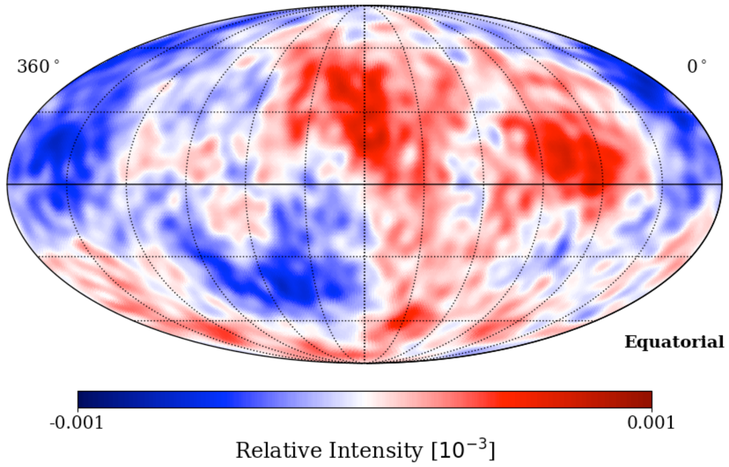
$$\tilde{C}_\ell = \frac{1}{2\ell+1} \sum_{m=-\ell, m\neq 0}^{\ell} |\hat{a}_{\ell m}|^2$$

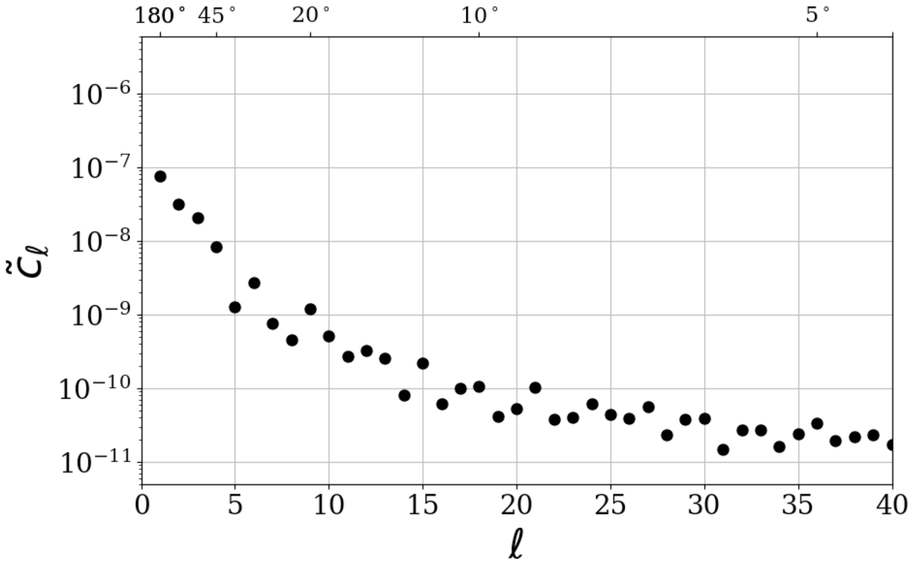
Original distribution





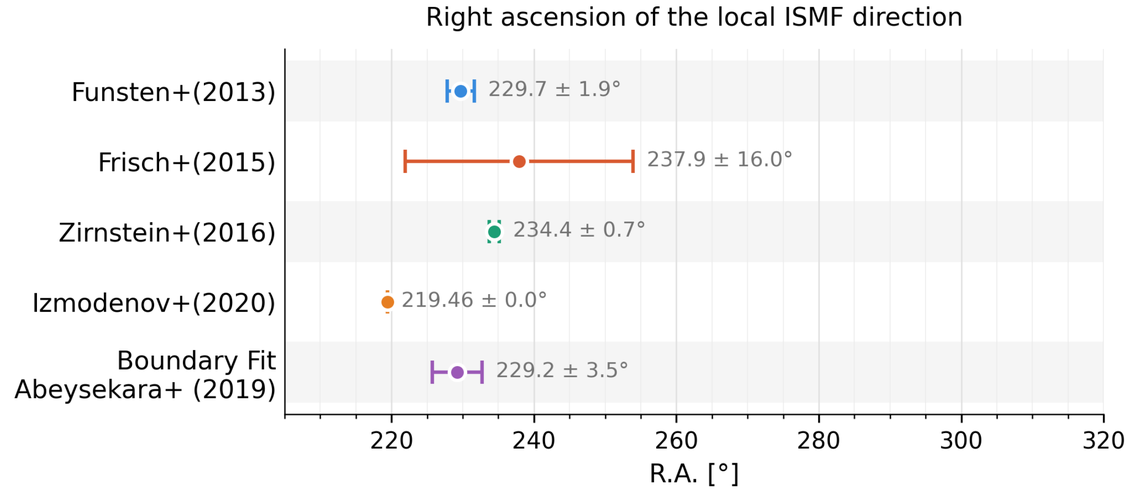
Observational bias (missing m=0)

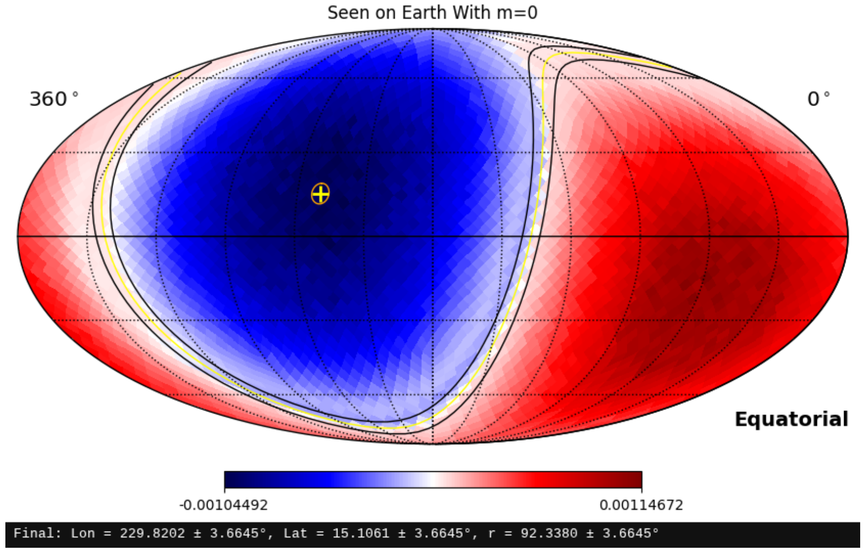


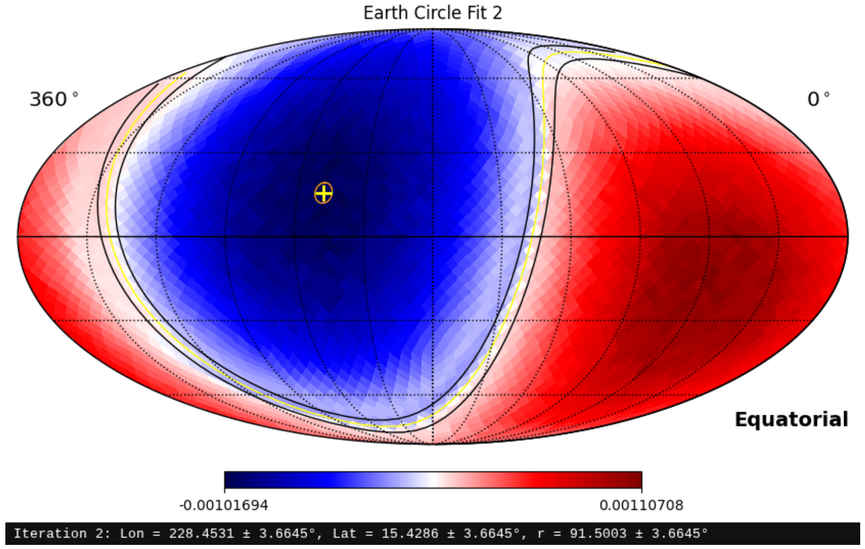


Estimating the amplitude of the ℓ=1,m=0 term.

- Higher multipoles describe the magnetic equator even in the absence of m=0 terms.
- This region has the steepest gradient in the relative intensity.
- Fitting a great circle to the max gradient provides an estimate of the direction of the LIMF.
- Assuming the dipole is oriented in this direction, we can estimate the δ_{N} term.





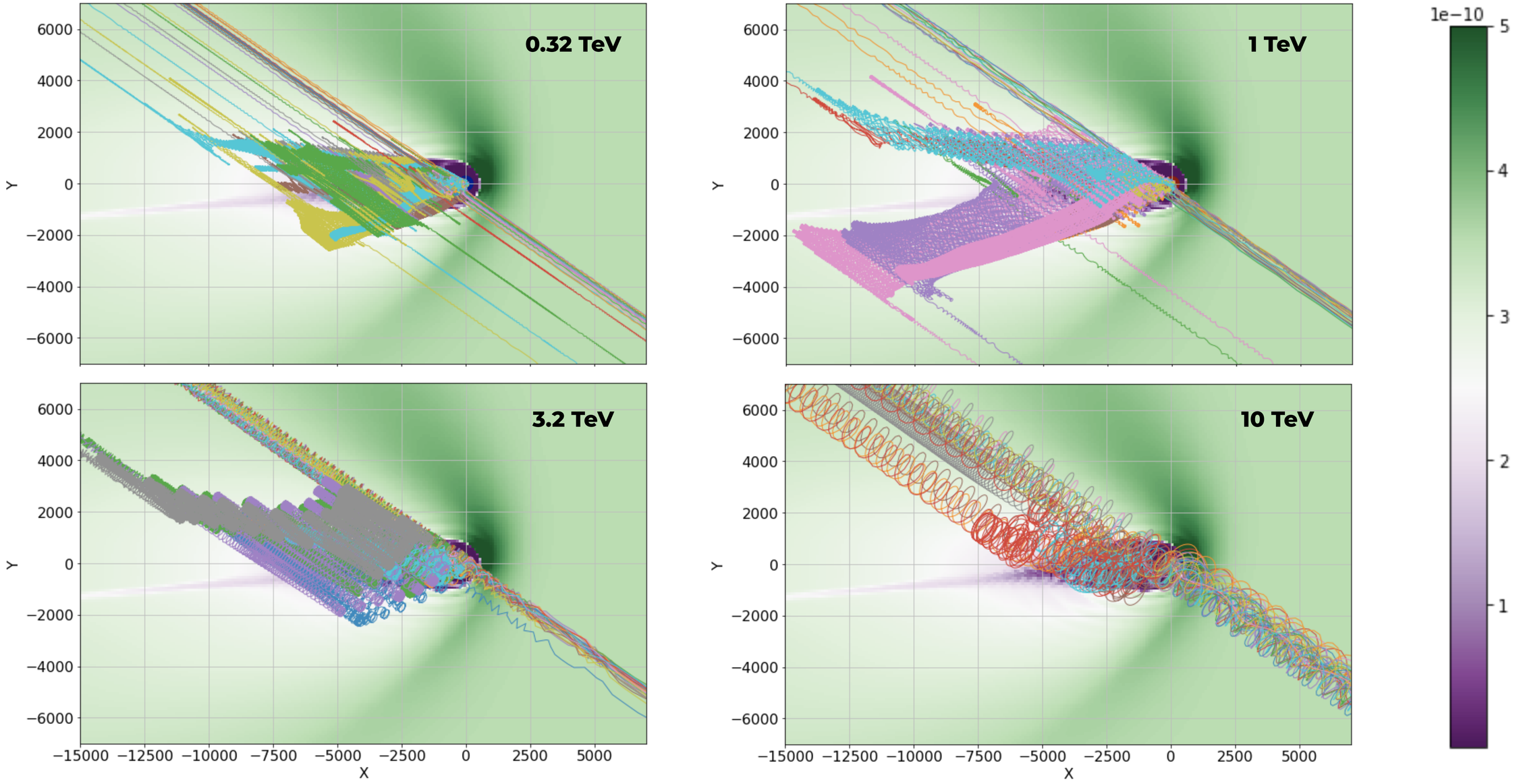


Simulation

J. C. Díaz-Velez, P. Desiati

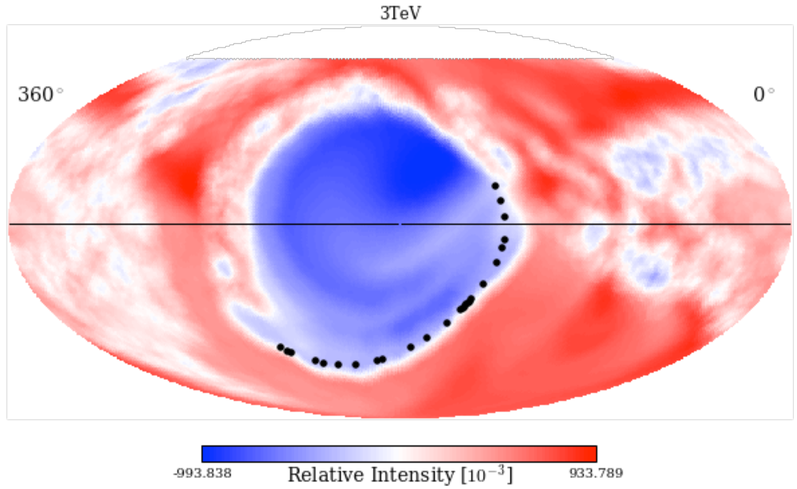
Heliospheric model: Pogorelov et al.(2015)

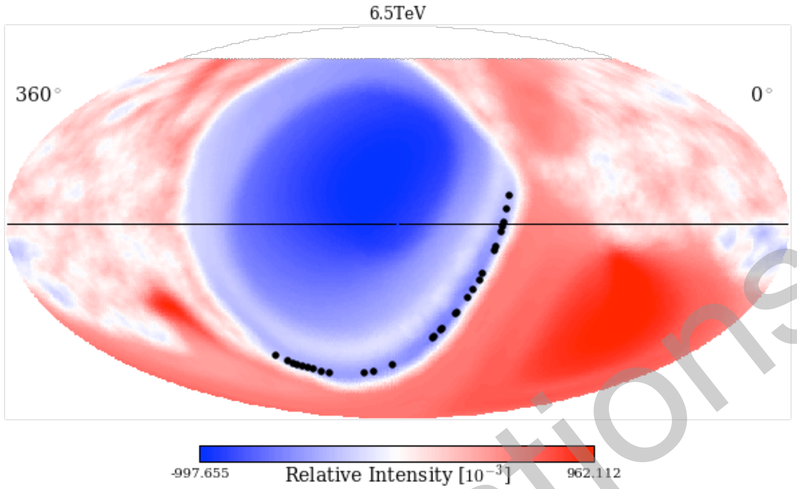
TeV Cosmic Rays in the Heliosphere

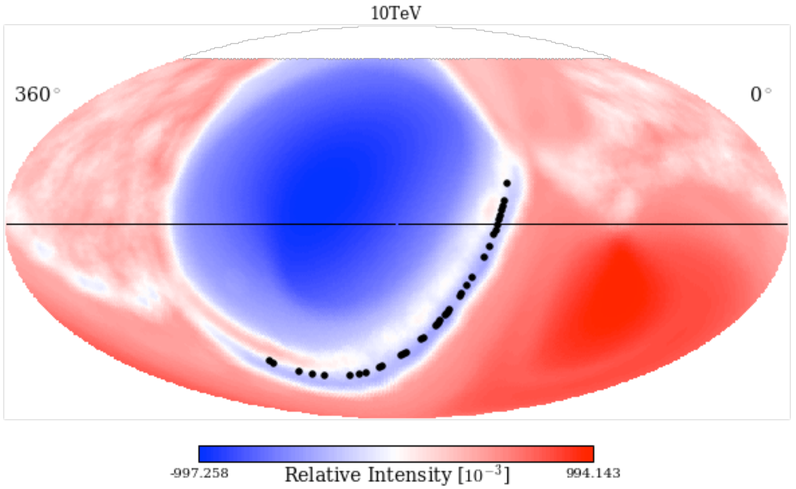


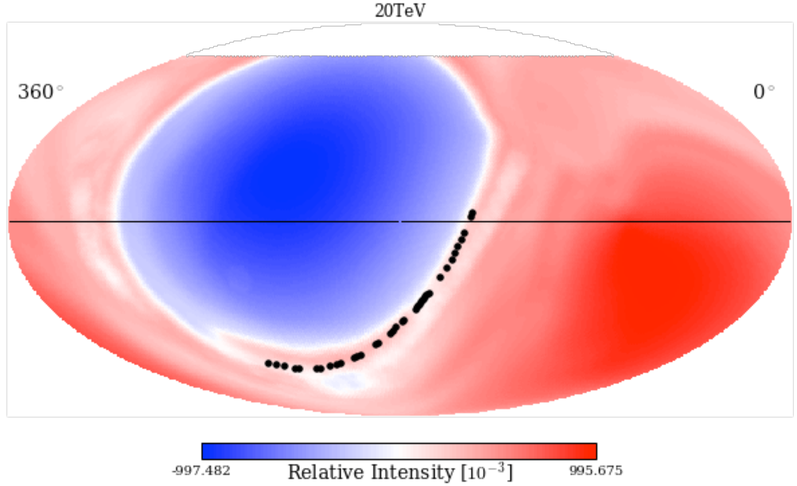
Anisotropy as a Function of Energy (Model)

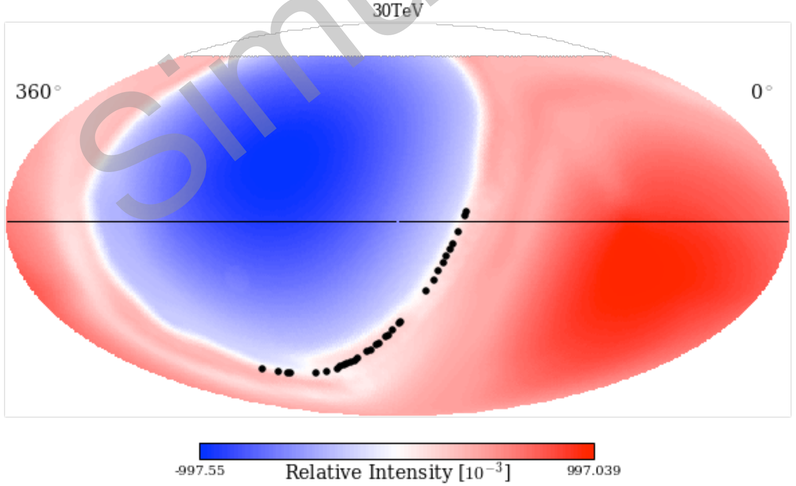
J. C. Díaz-Velez, P. Desiati

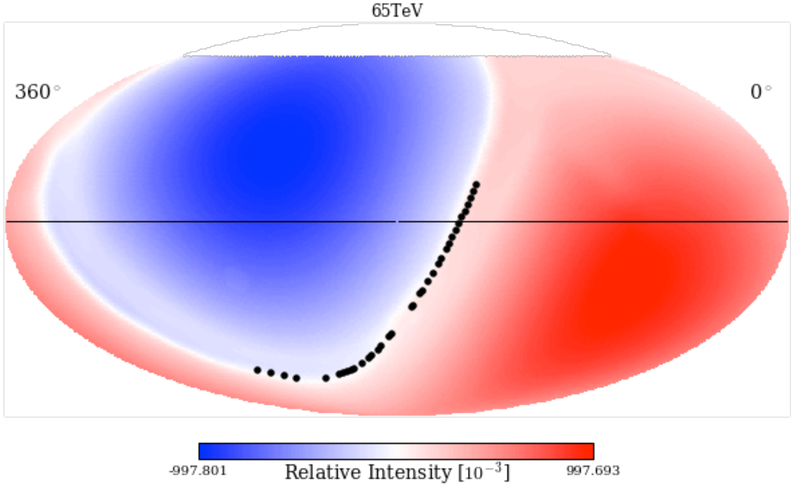








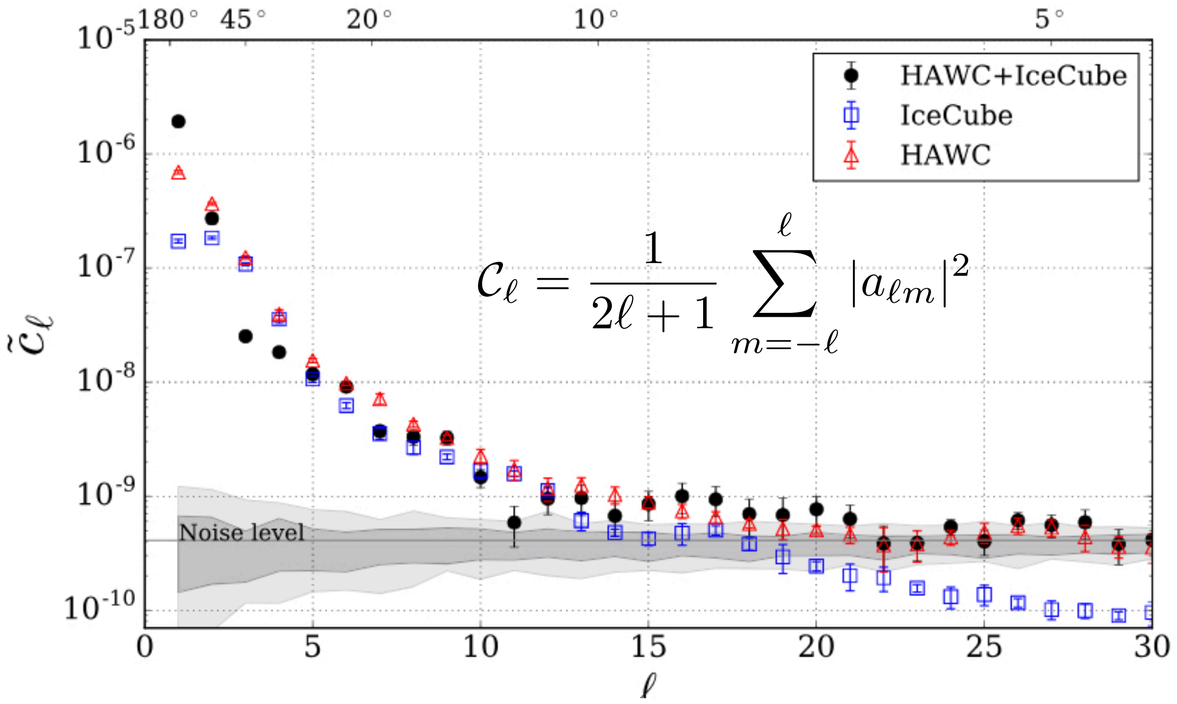




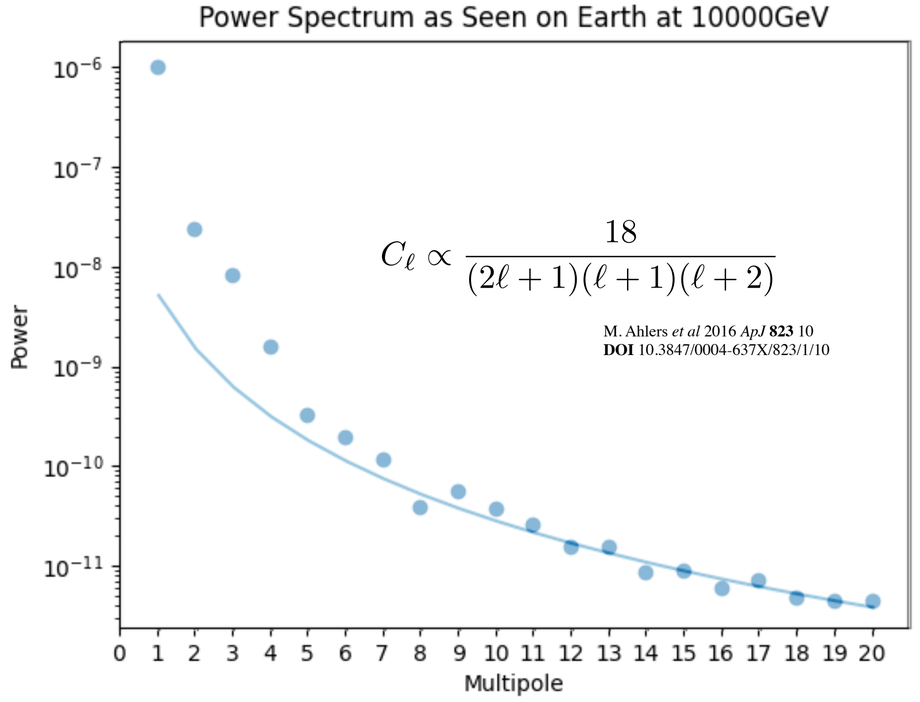
Simulations

Angular Power Spectrum

M. Ahlers: Simple model of hierarchical structure of c_ℓ arising from the local turbulence of B-fields: higher multipole moments are induced locally by a global diffuse dipole moment within times Tv ≲ 1. Expect strength of individual multipoles to decreases in time.



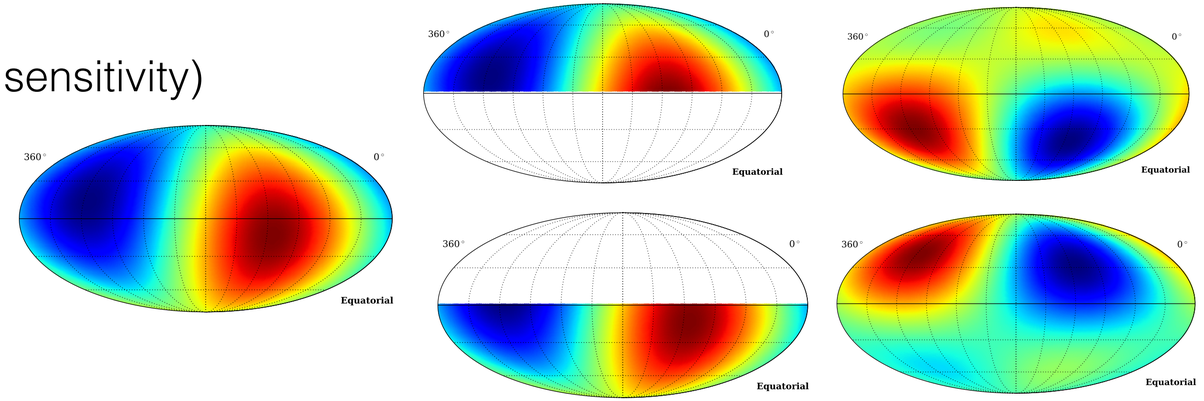
A. U. Abeysekara, et al. **DOI** 10.3847/1538-4357/aaf5cc



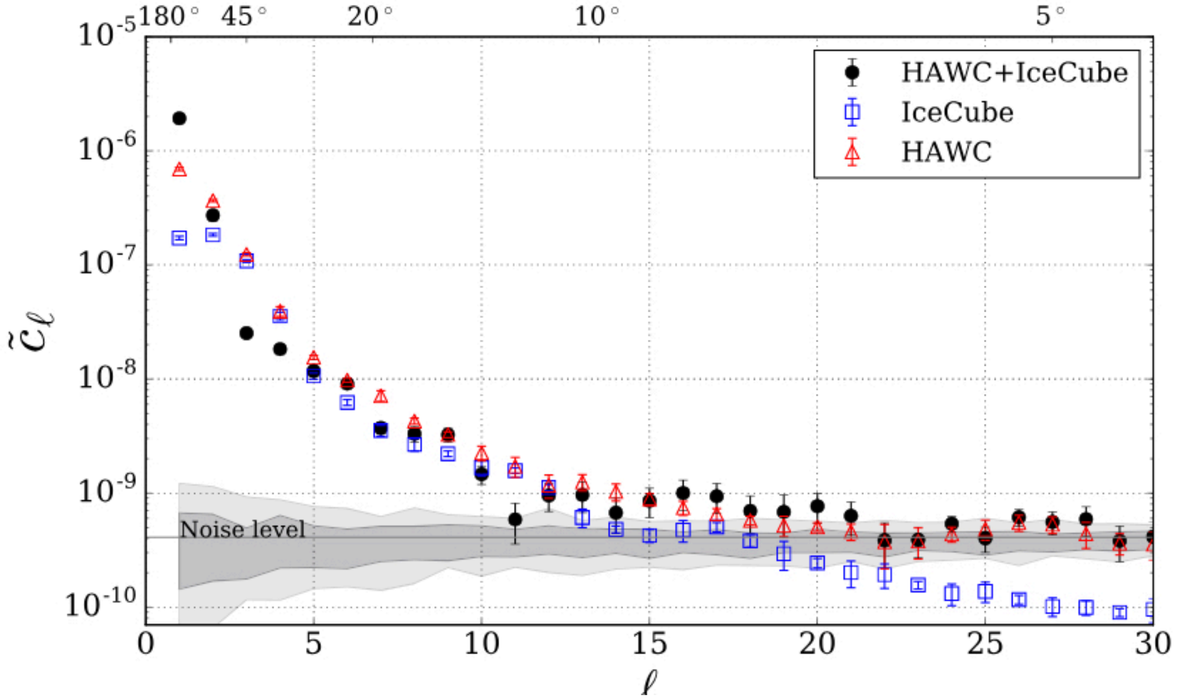
Simulation

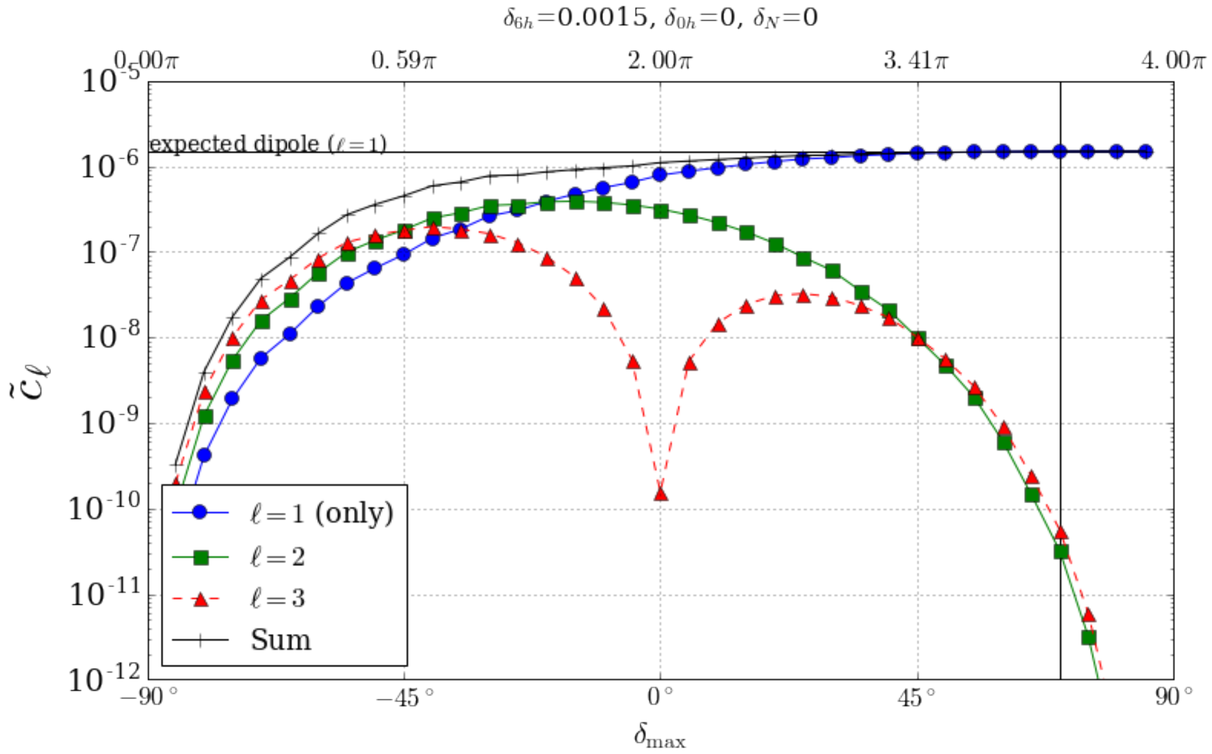
Observational bias: partial sky-coverage

Pure dipole (3d sensitivity)

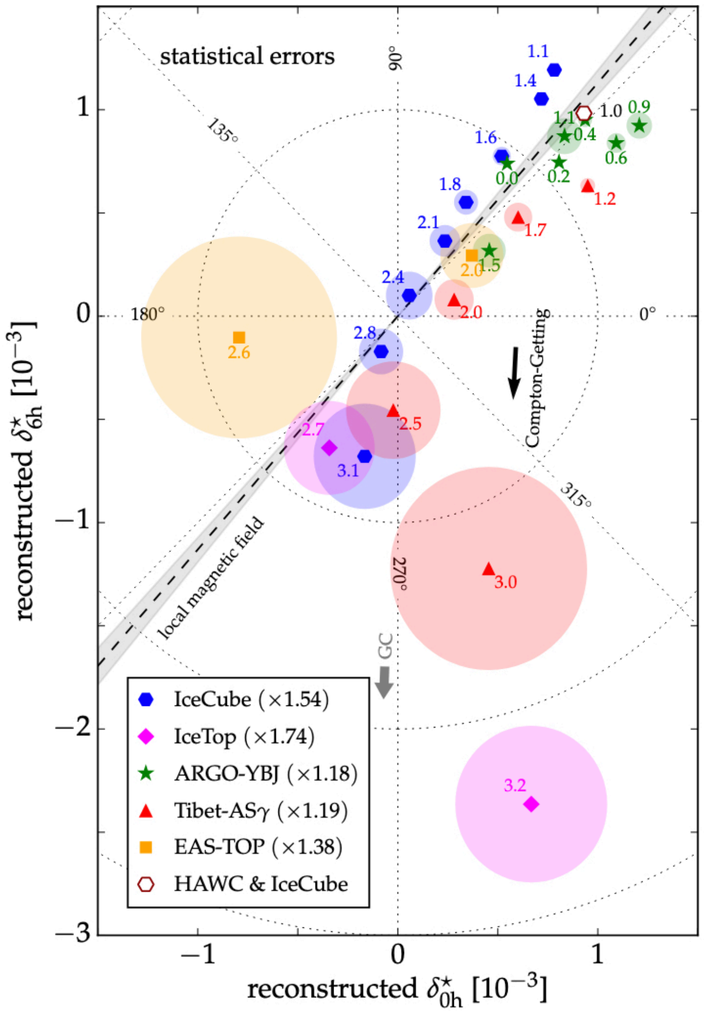


Multipole components are subject to crosstalk caused by partial sky coverage since there is a degeneracy between different ℓ-modes.
A purely dipole can result in an artificial quadrupole due to partial sky coverage.

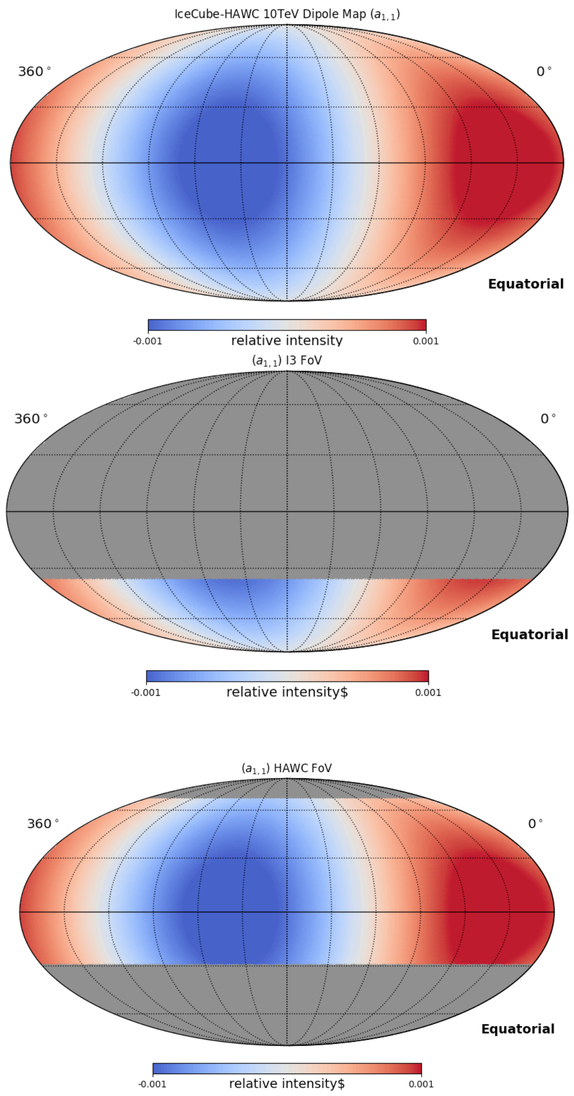




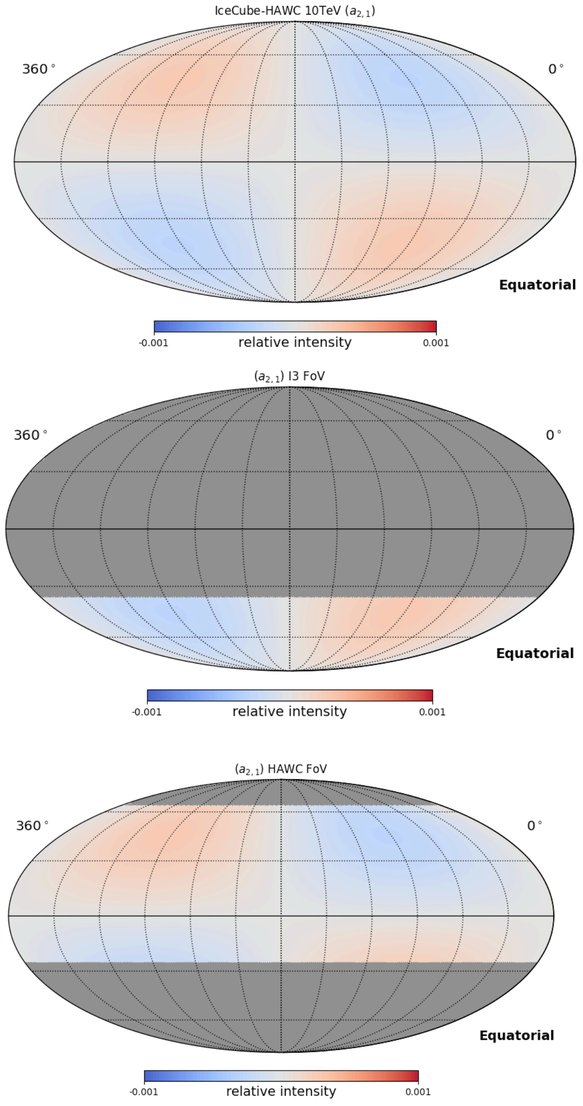
m=1 quadrupole biases dipole measurement for partial sky



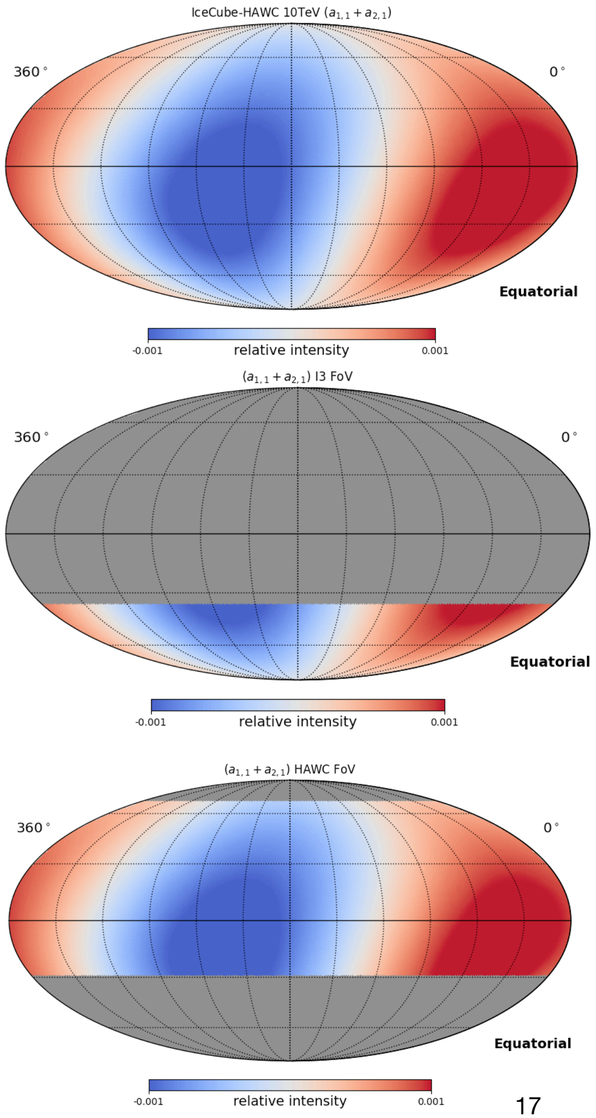
icecube: amplitude=0.0012, phase=38.3º
hawc: amplitude=0.0012, phase=38.3º



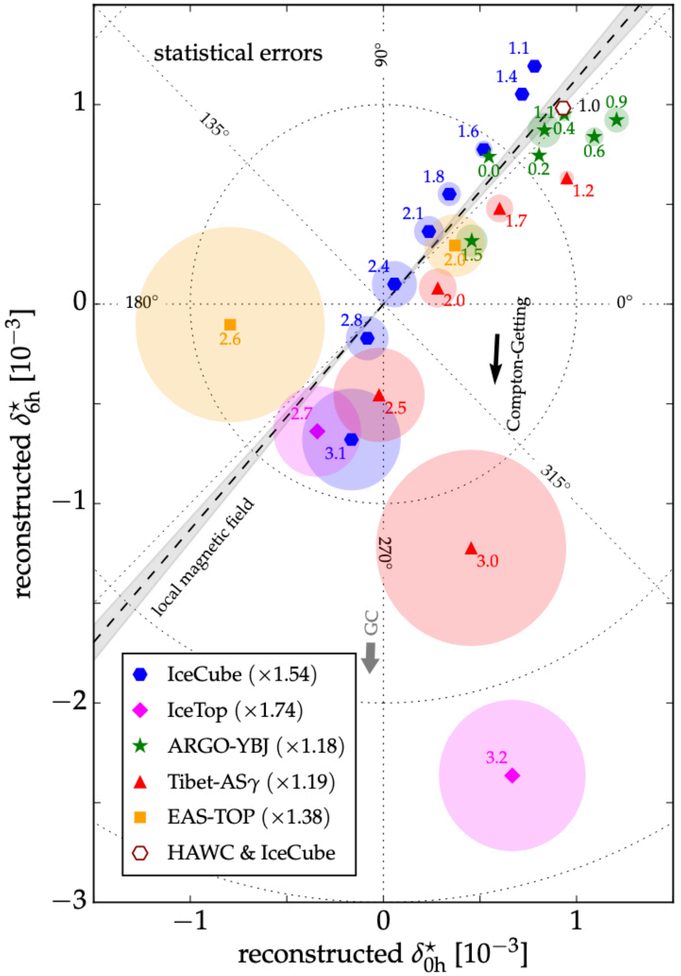
icecube: amplitude=0.00041, phase=93.3º
hawc: amplitude=8.5e-05, phase=273.3º

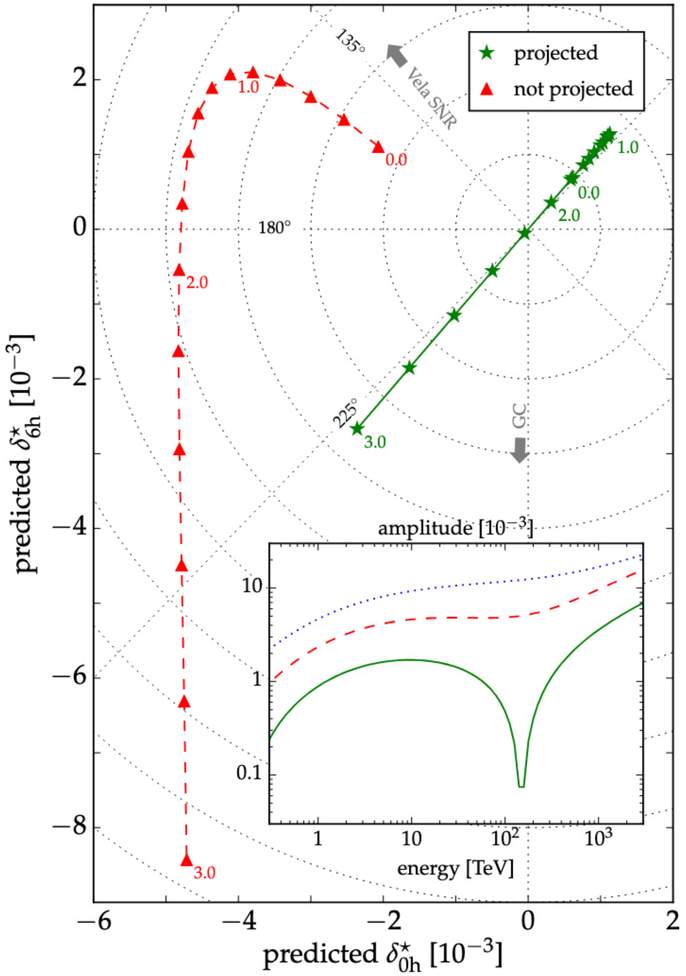


icecube: amplitude=0.0014, phase=51.7º
hawc: amplitude=0.0011, phase=35.4º



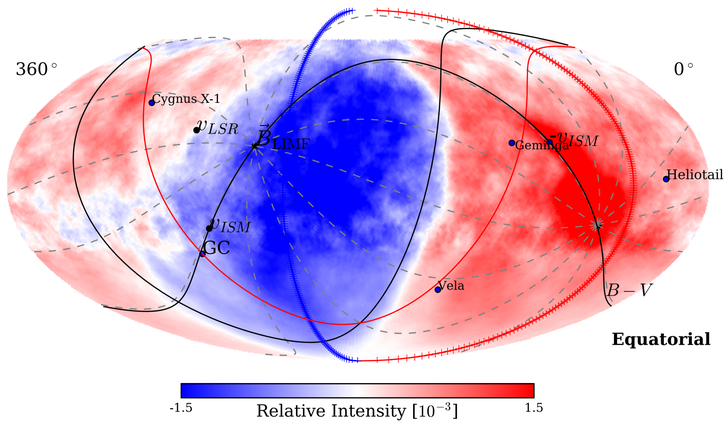
Possible Scenarios for Dipole Evolution





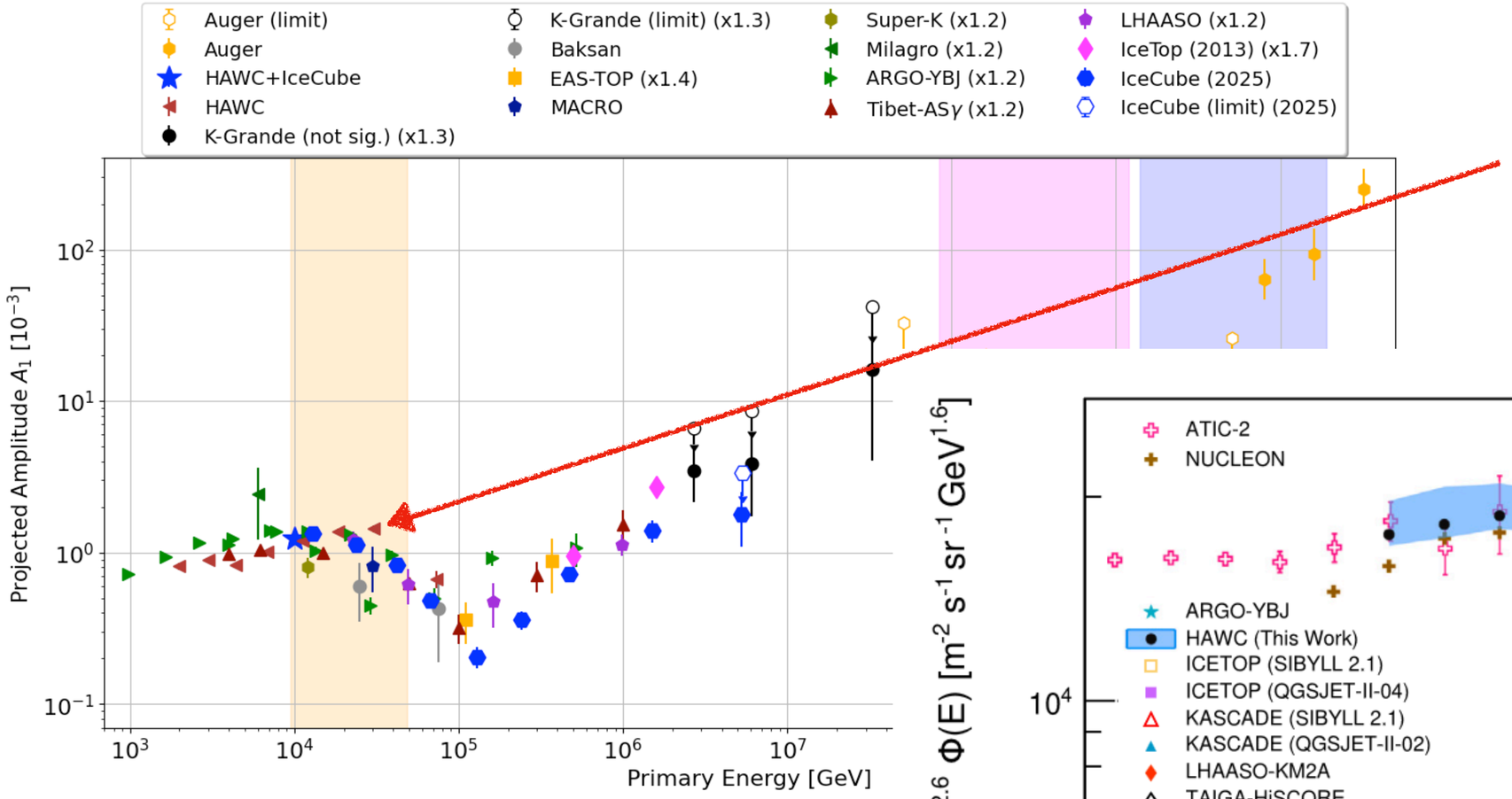
Left Panel: Reconstructed TeV–PeV dipole component in the equatorial plane.

Right Panel: Predicted dipole anisotropy in a model that accounts for the contribution of local SNRs.

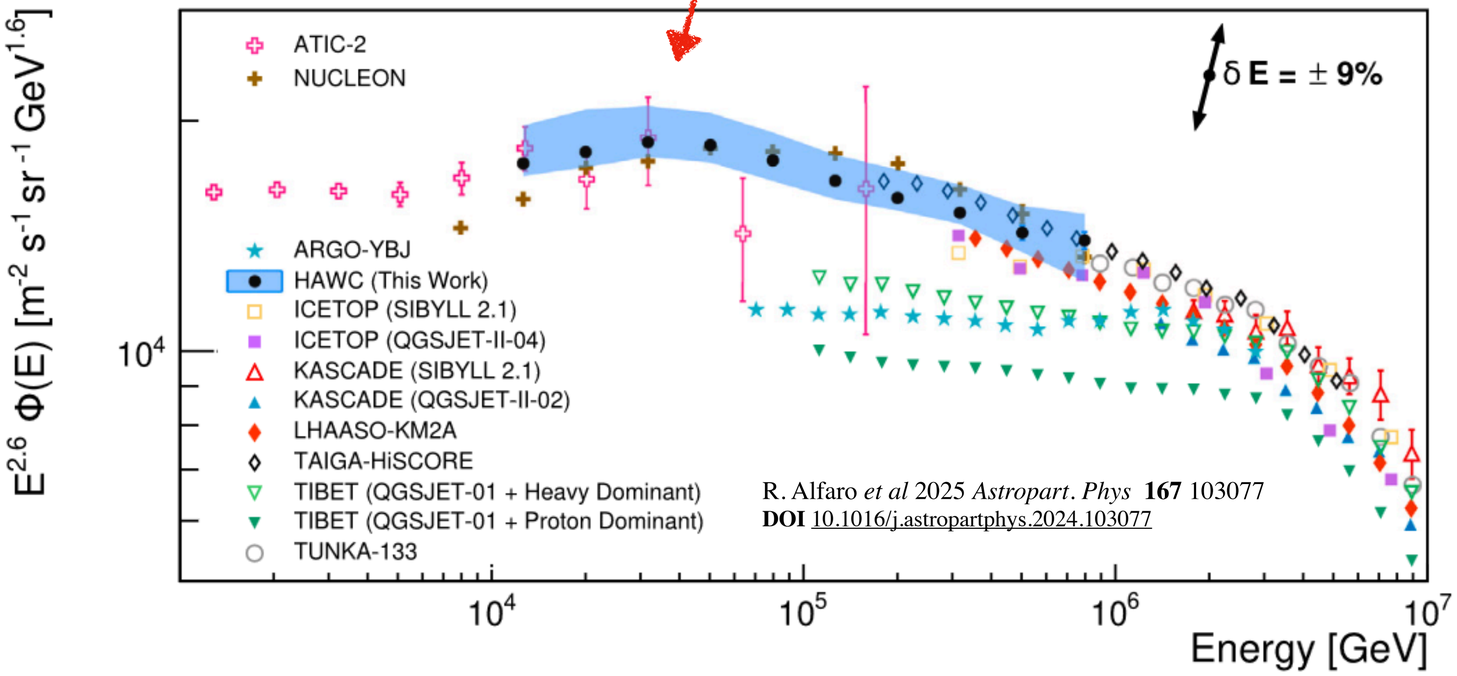


Markus Ahlers 2019
J. Phys.: Conf. Ser. 1181 012004

Dipole Component vs. Energy



Softening of spectrum & dipole amplitude



Reconstructed amplitude of the horizontal c
Bands represent the range of gyroradii for the
cloud, and the local bubble, including B-fields i
median lnA from GSF.

HAWC all-particle spectrum of cosmic-rays

APS vs Energy

- APS reflects the redistribution of power from small ℓ to higher multipoles observed in maps as a function of energy.
- Dipole is no longer dominant structure above 200 TeV

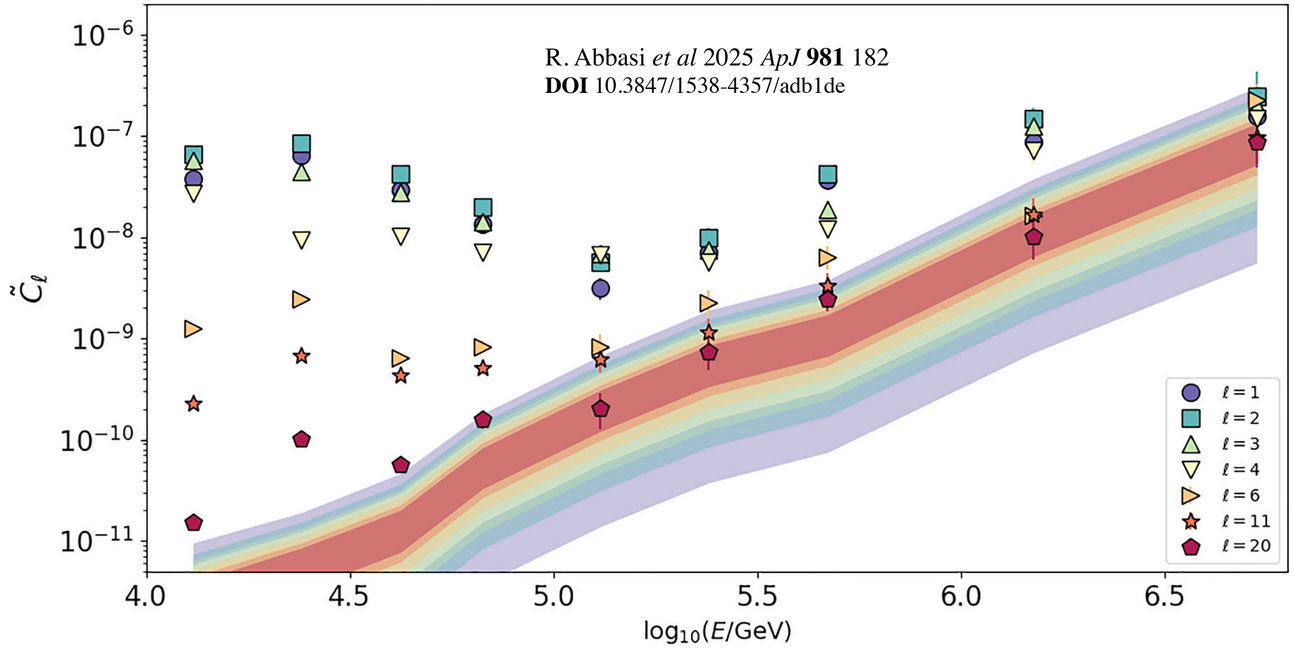
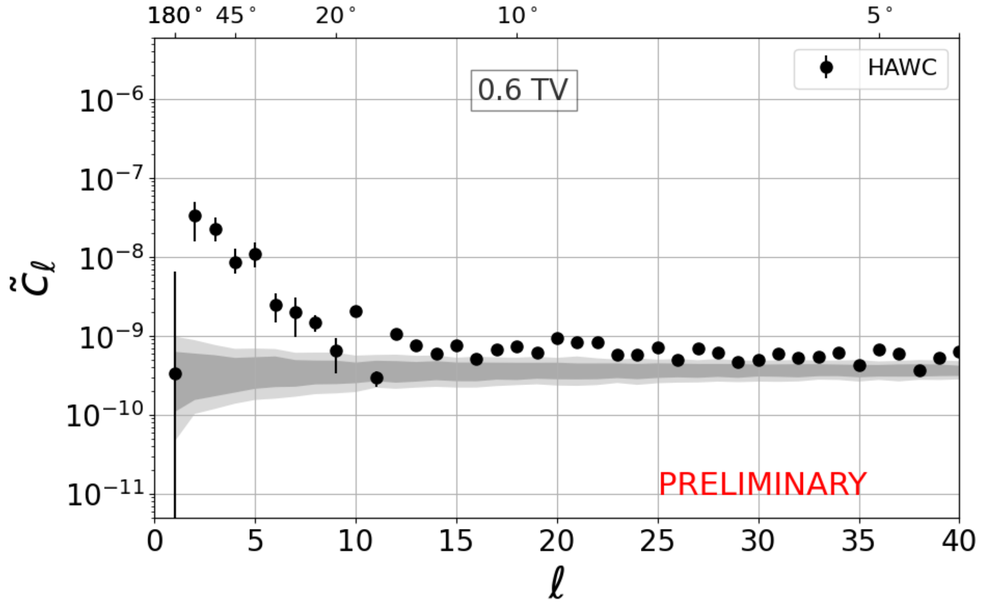
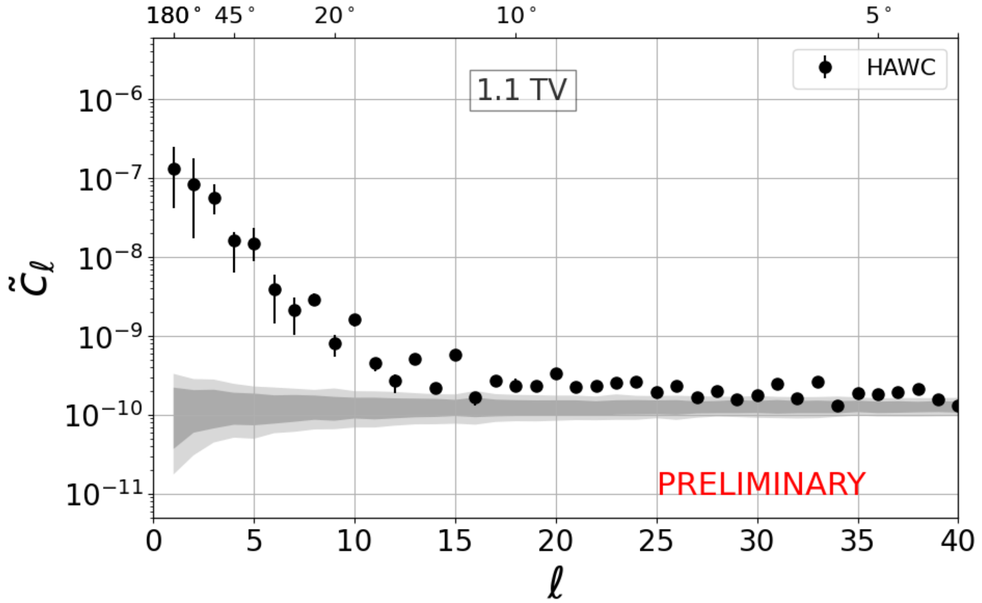
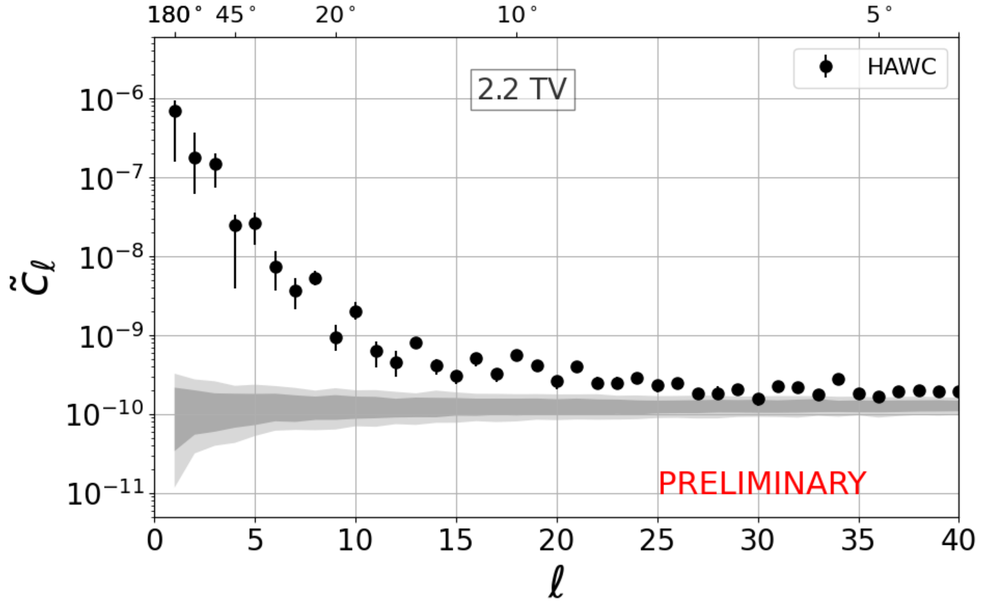


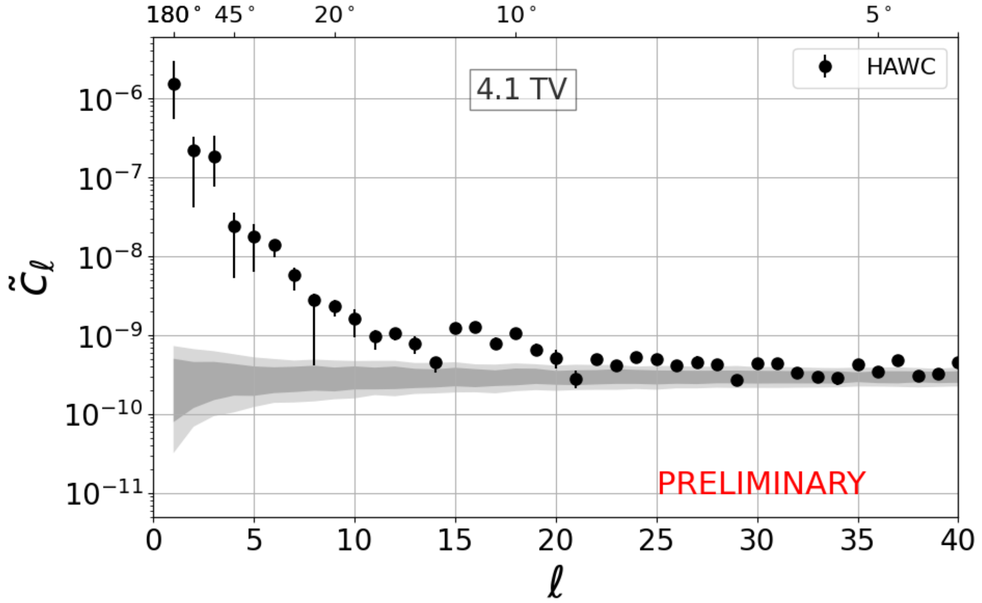
Figure 7. Angular pseudo-power for selected spherical harmonic modes (ℓ) as a function of median primary energy for 12 yr of IceCube data. Errors bars are statistical. The bands indicate the 95% spread in from a large sample of scrambled maps. The color of the bands corresponds to that of the data symbols but in a lighter shade.

Angular Power Spectra

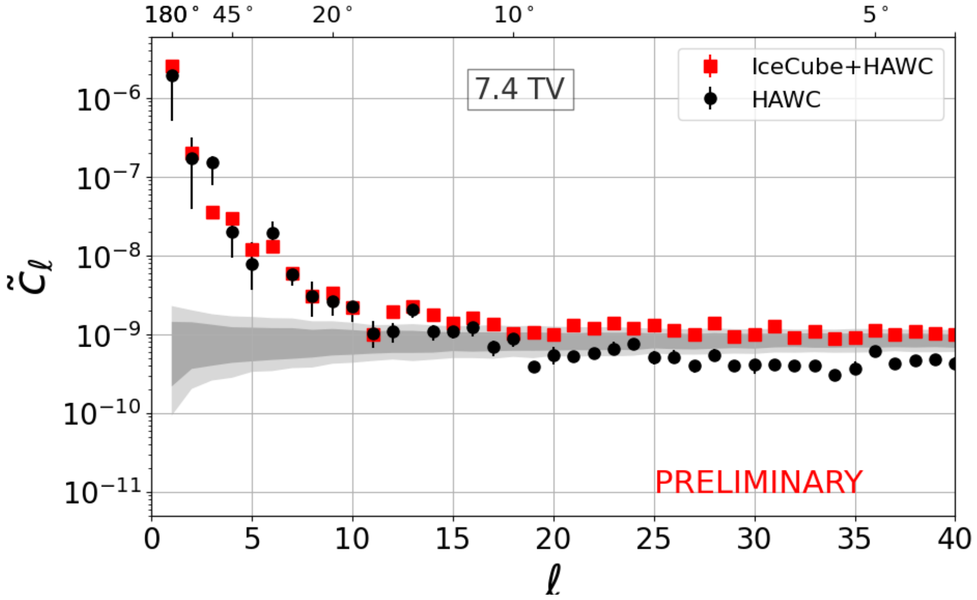


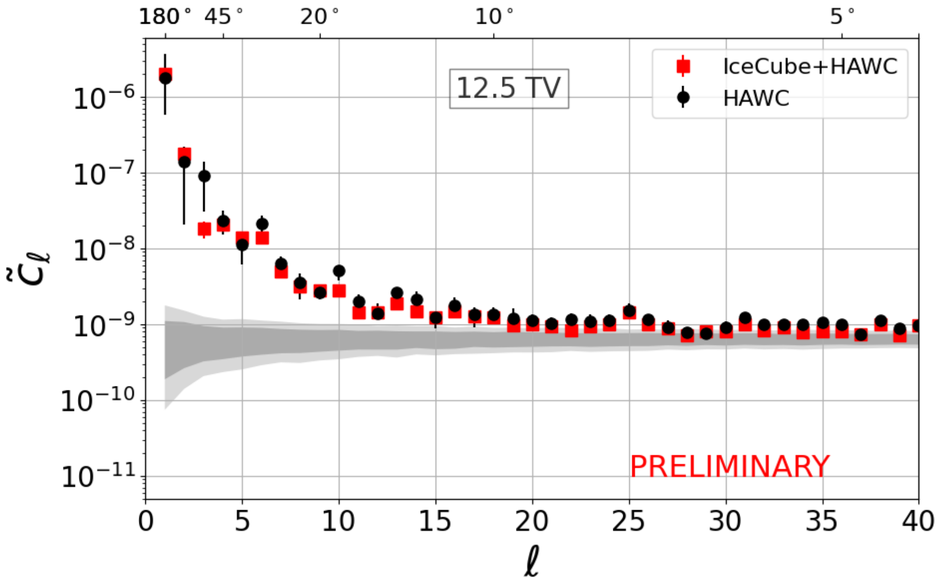


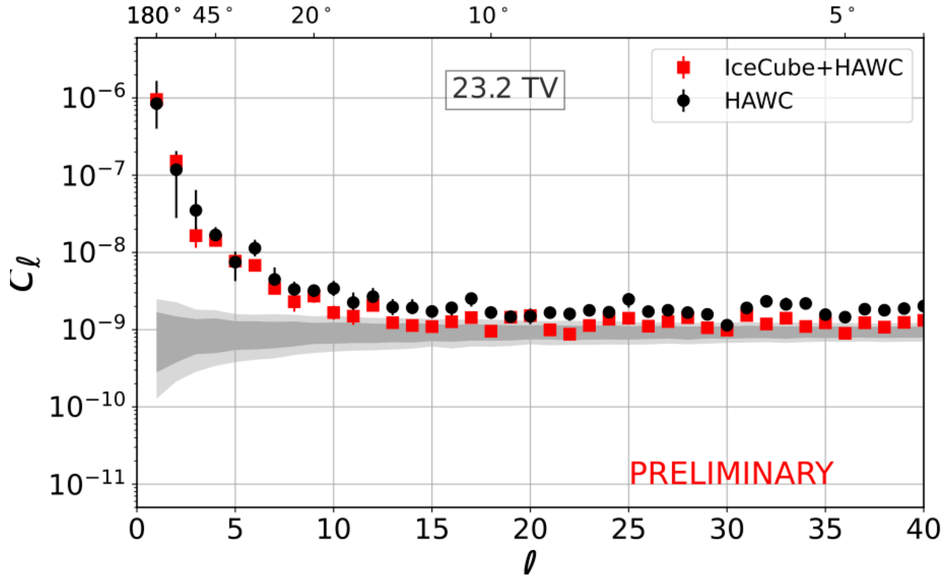


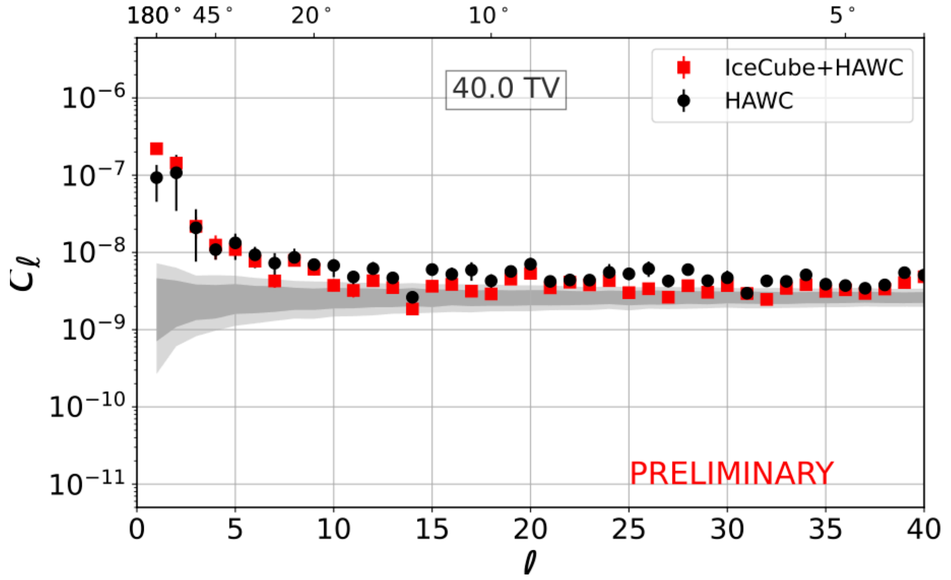


Angular Power Spectra

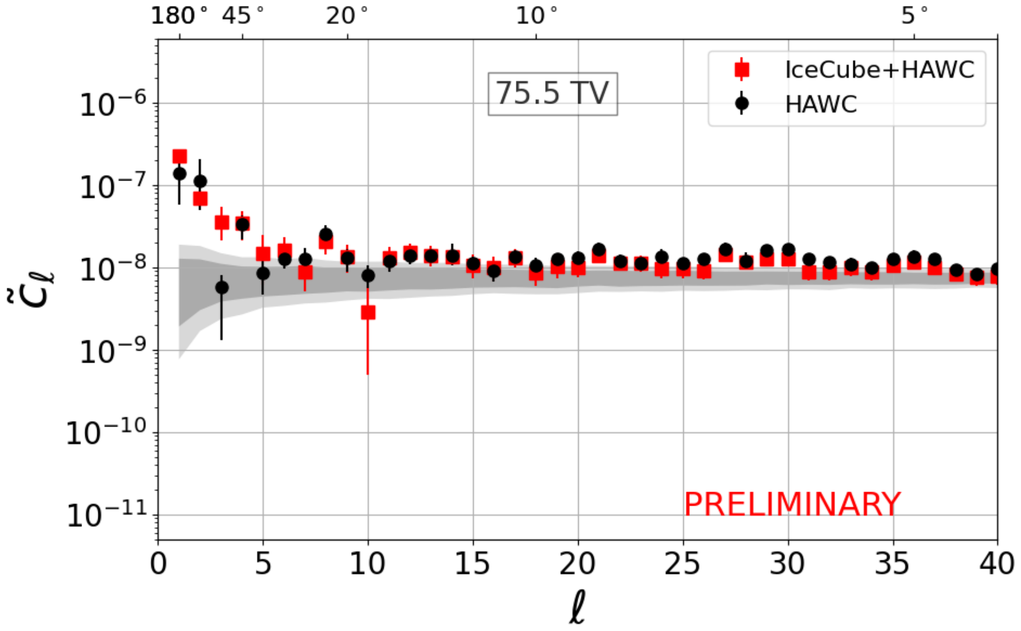


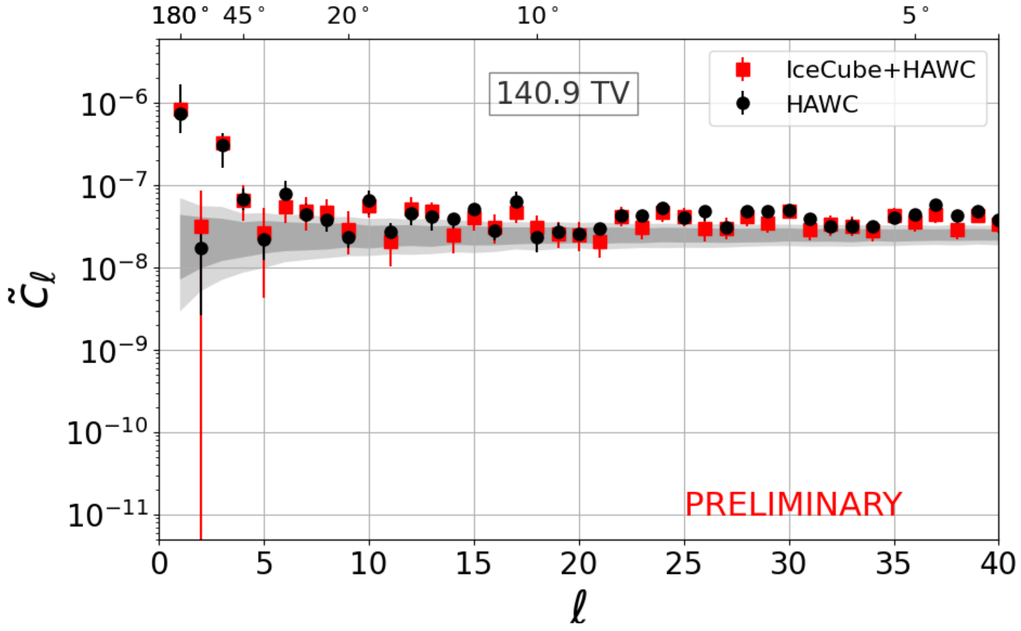


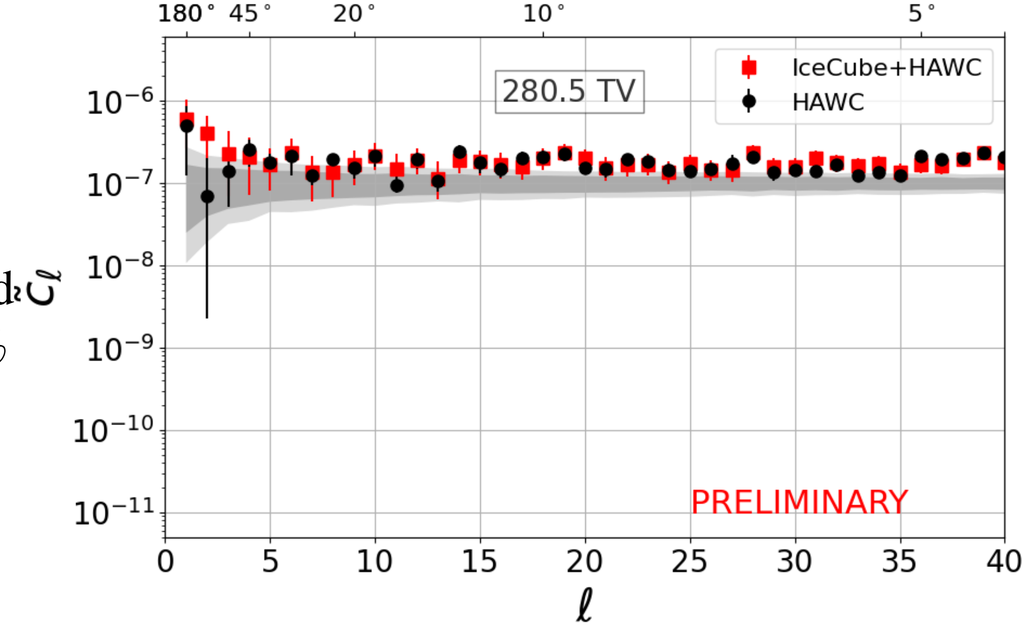




HAWC & IceCube PoS(ICRC2025)244



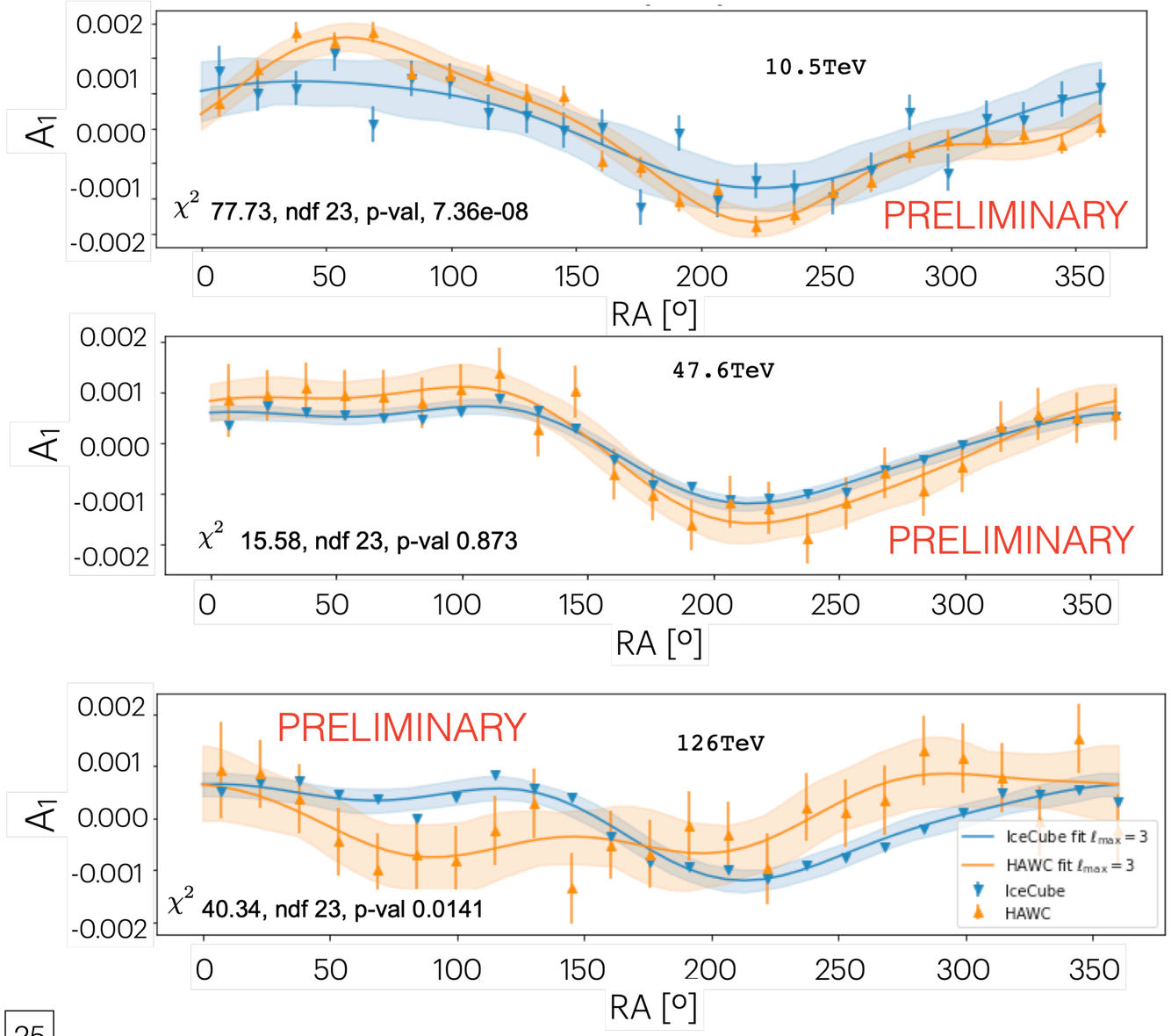




Combined angular power spectra for 11 rigidity-driven pairs of energy bins. Error bars represent statistical uncertainties. Shaded regions correspond to the isotropic noise at 68% (dark) and 90% (light) confidence intervals.

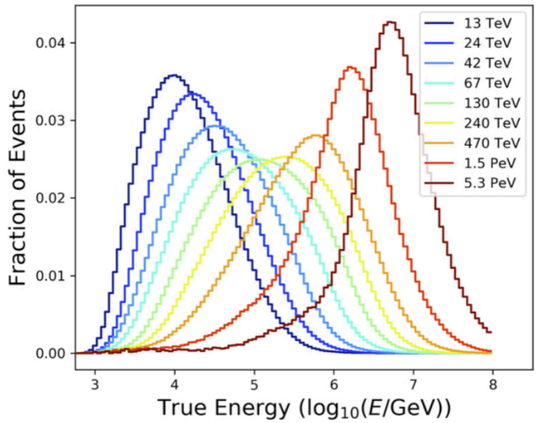
Rigidity Dependent Anisotropy

Overlapping Region

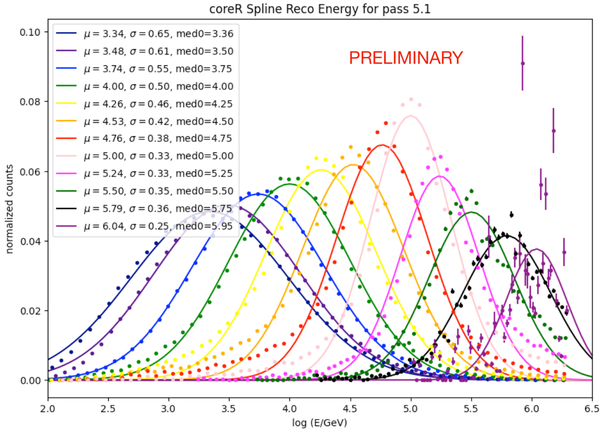


- At ~50 TeV data are statistically compatible in the overlapping region
- Tension between measurements at 10 TeV and 126 TeV

IceCube Energy Bins



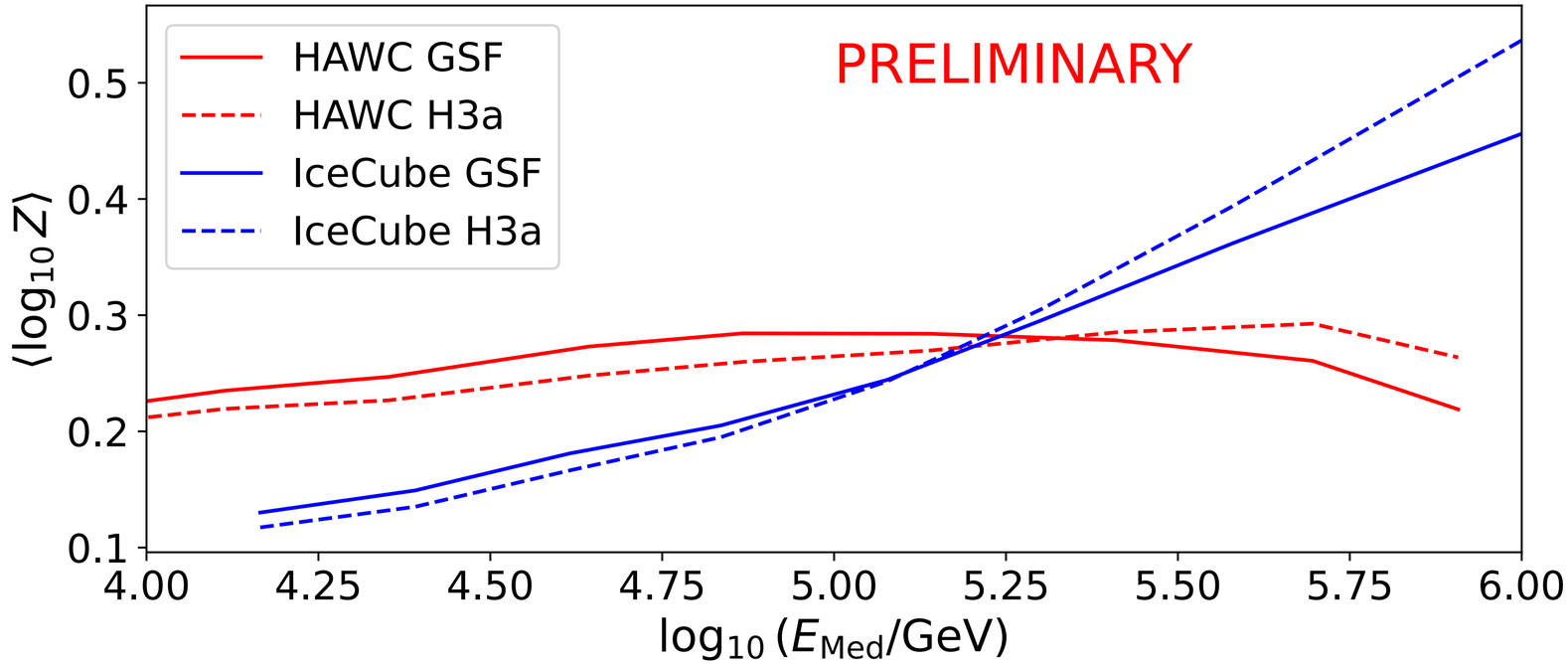
HAWC Energy Bins



Abbasi, R., et al (2025). ApJ *981*(2), 182-.
https://doi.org/10.3847/1538-4357/adb1de

HAWC & IceCube PoS(ICRC2025)244

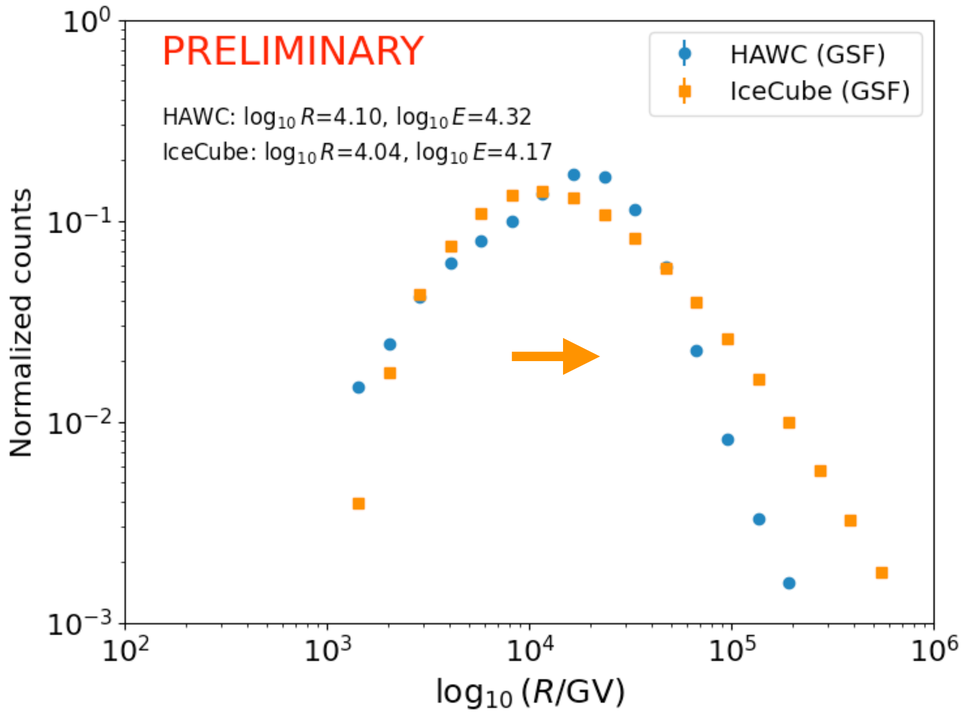
Composition Assumptions

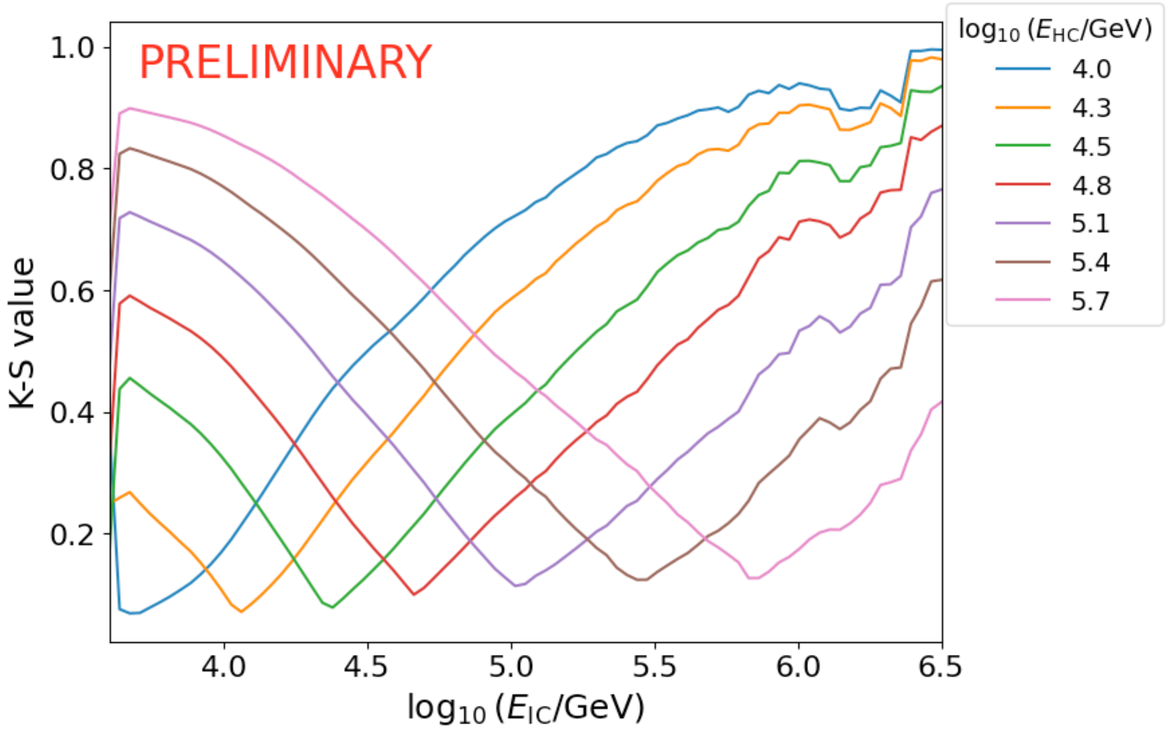


- Mean logarithm of the particle charge Z for cosmic rays detected by IceCube (blue) and HAWC (red) assuming the Gaisser H3a [T. K. Gaisser Astropart. Phys. 35 (2012) 801–806] (dashed) and GSF [H. Dembinski, et al. PoS ICRC2017 (2017) 533] (solid) composition models.

- IceCube data is dominated by protons and light elements at lower energies than HAWC, but becomes heavier above about 200 TeV.

Composition Assumptions

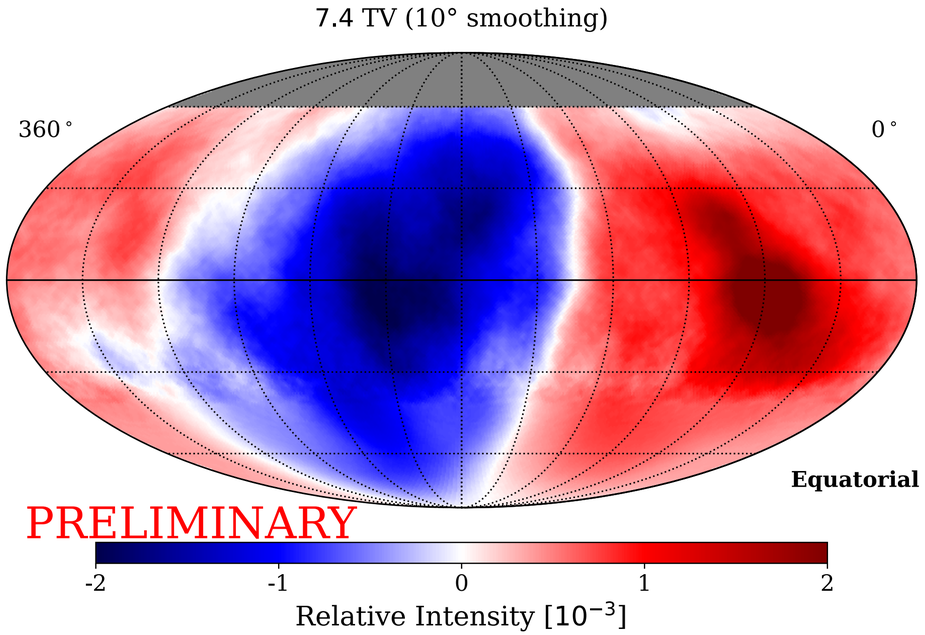


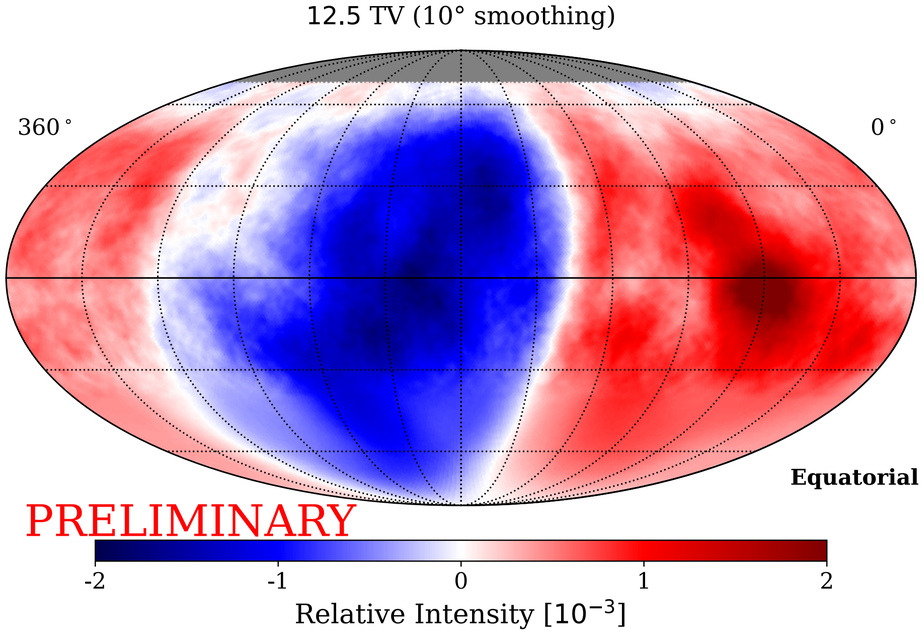


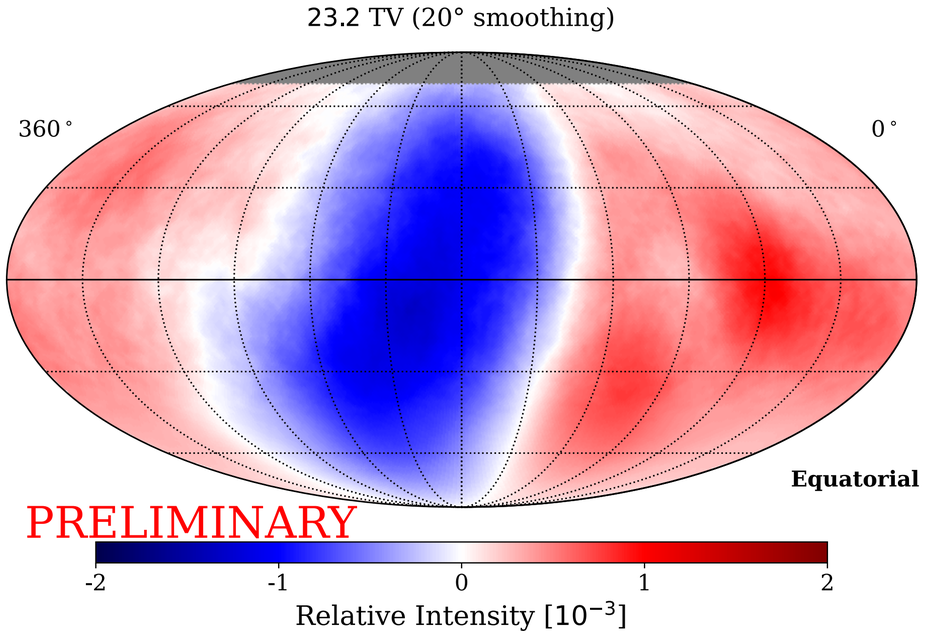
Slide IceCube window and minimize K-S test between rigidity distributions

Assuming a rigidity–dependent angular distribution of cosmic rays, we find the most compatible energy bins by sliding an IceCube energy window of size Δ log10 E = 0.25 and minimizing the K-S test value between rigidity distributions based on Monte Carlo simulations.

Combined Relative Intensity





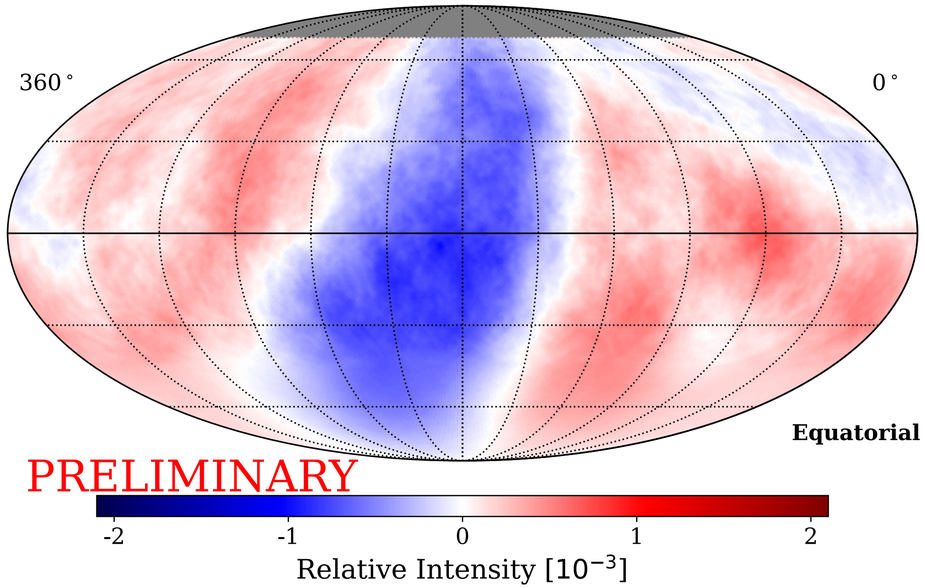


Relative intensity for rigidity-driven pairs of energy bins. Combined relative intensity maps are reconstructed using the maximum likelihood method of [M. Ahlers et al 2016 ApJ 823 10]. A rapid phase transition is observed going from 40 TV to 76 TV consistent with previous individual measurements.

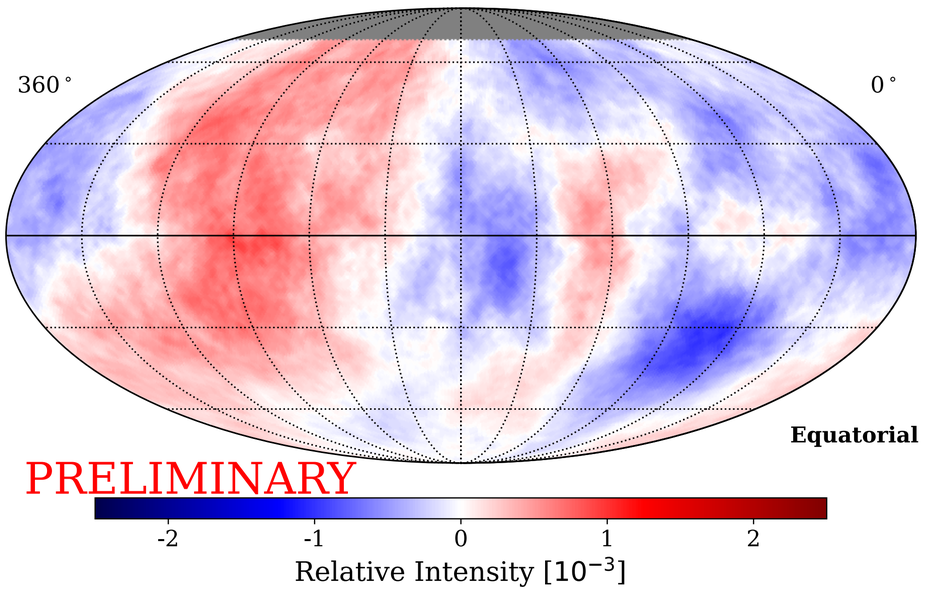
Combined Relative Intensity

HAWC & IceCube PoS(ICRC2025)244

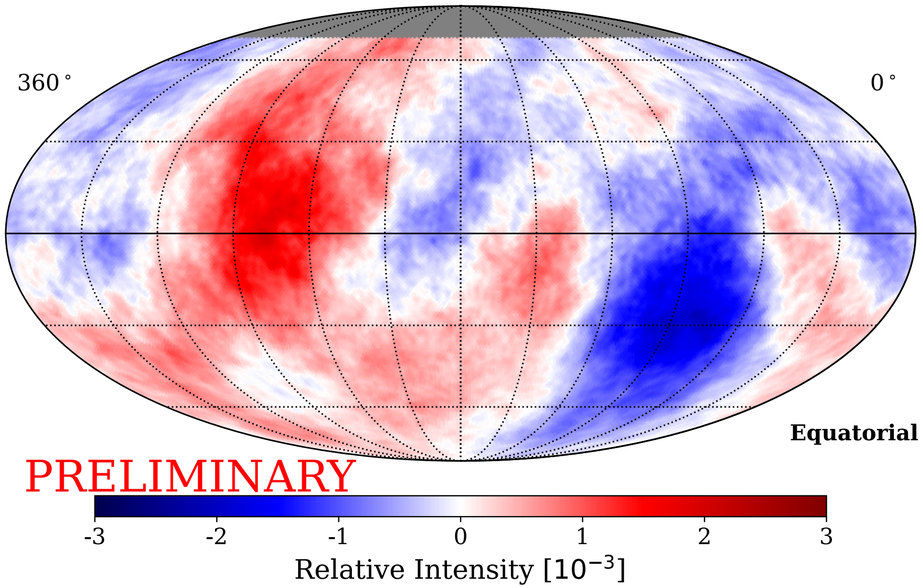
40.0 TV (20° smoothing)



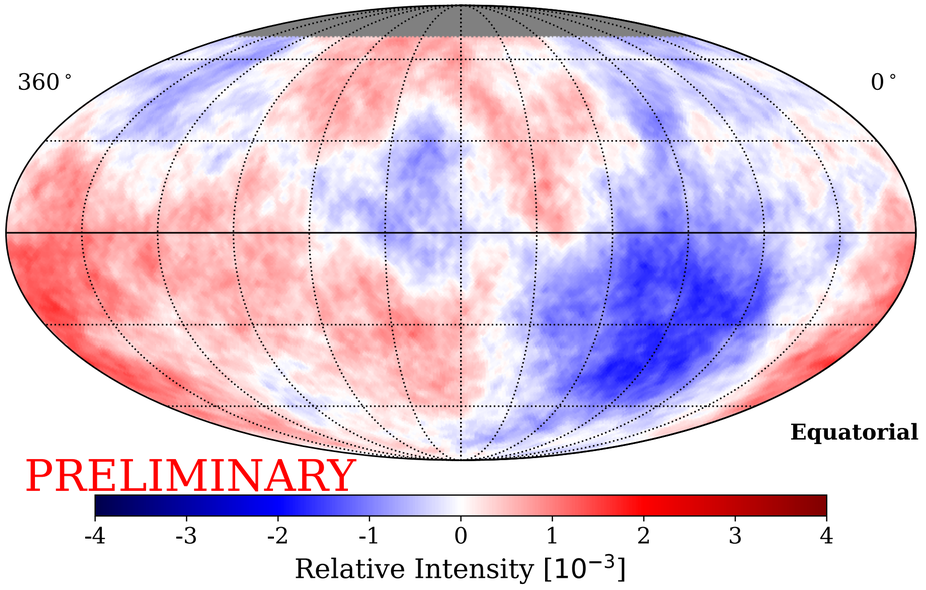
75.5 TV (20° smoothing)



140.9 TV (20° smoothing)



280.5 TV (30° smoothing)



LHASSO (KM2A) Proton Anisotropy

LHASSO PoS(ICRC2025)286

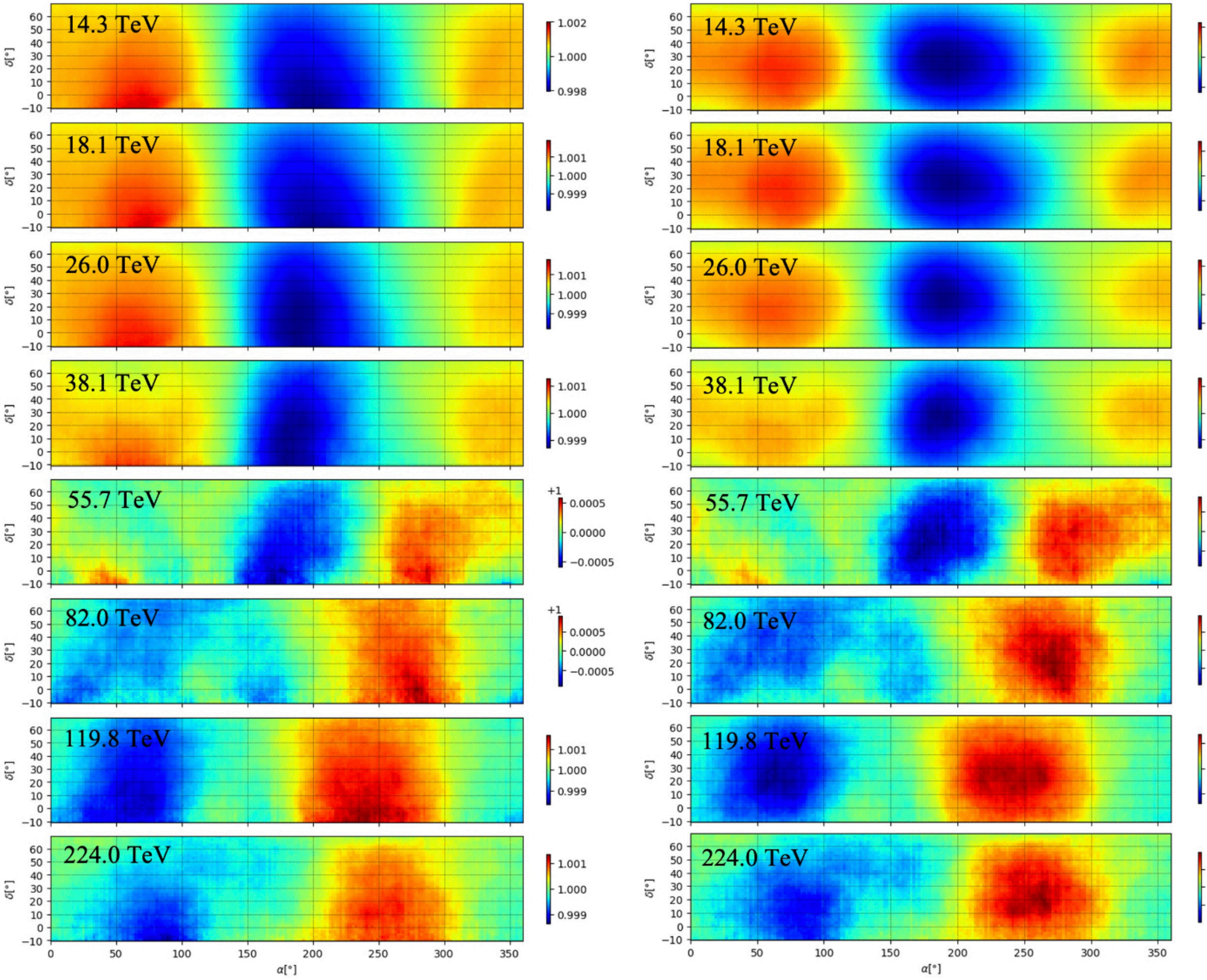
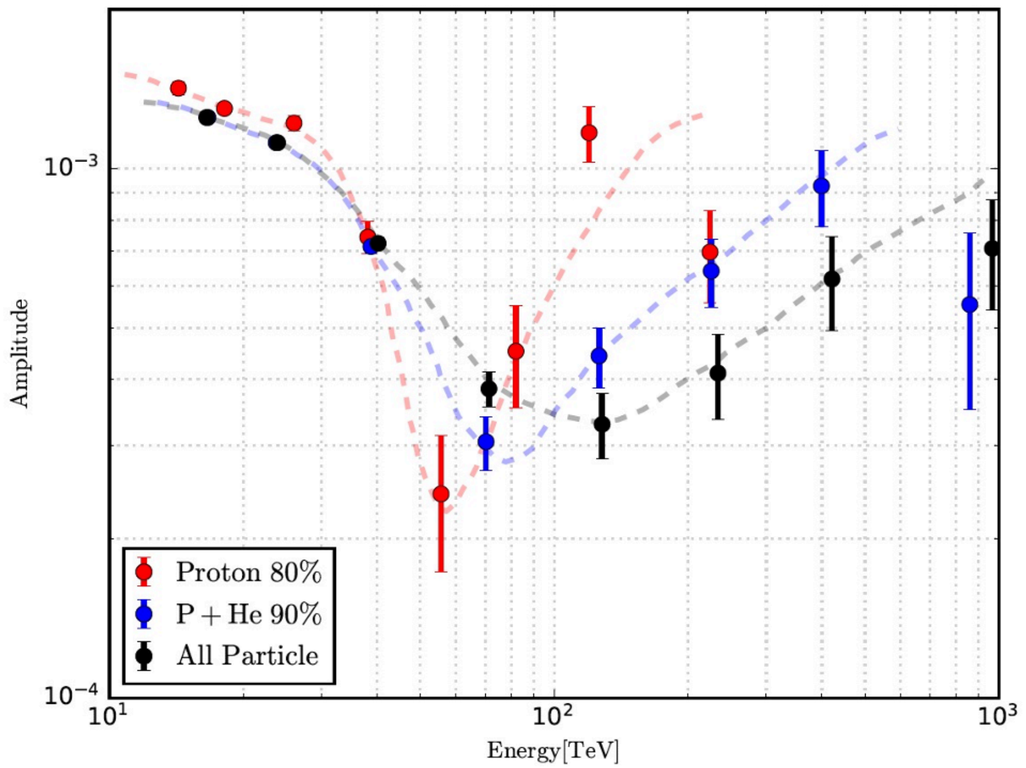
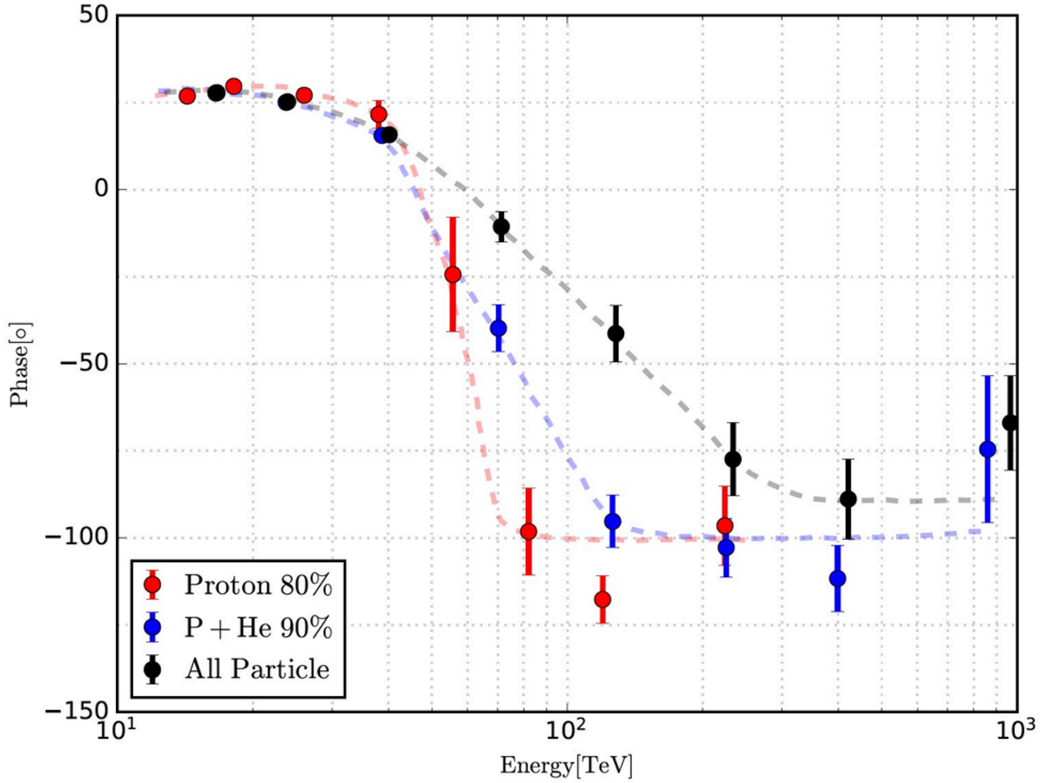
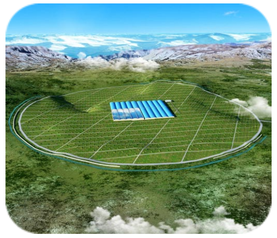


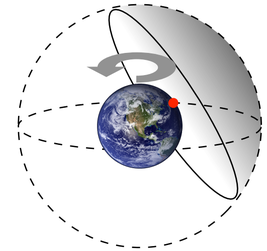
Figure 2: Sky maps of relative intensity (left) and significance (right) for proton-like samples. The maps have been smoothed with at 30° top-hat function.

Composition anisotropy: rigidity scaling?





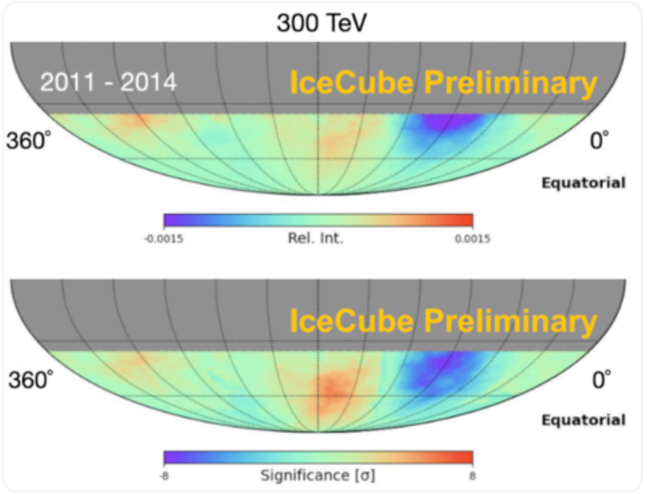


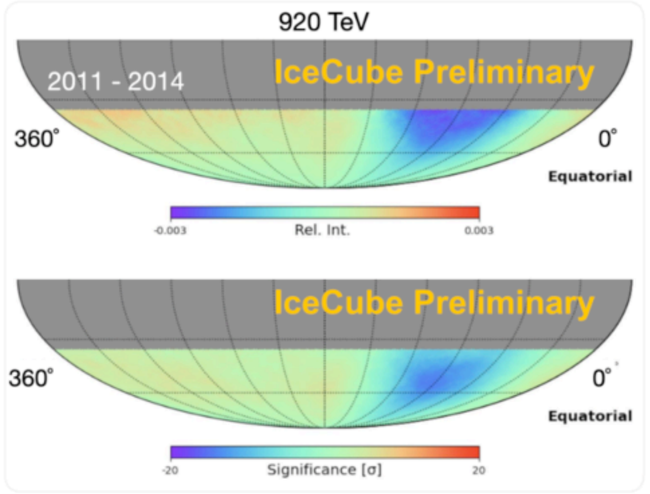


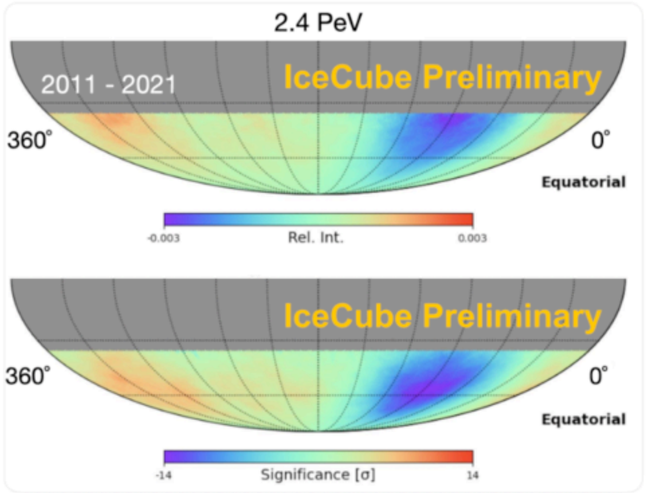
LHAASO
PoS(ICRC2025)286

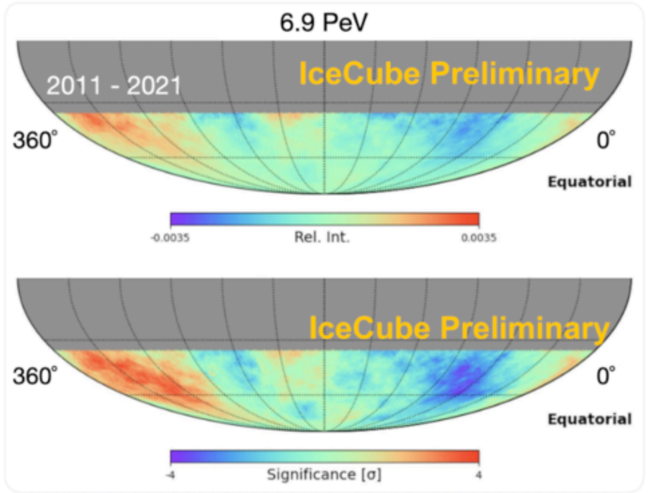
Mass selection and composition sensitivity are crucial

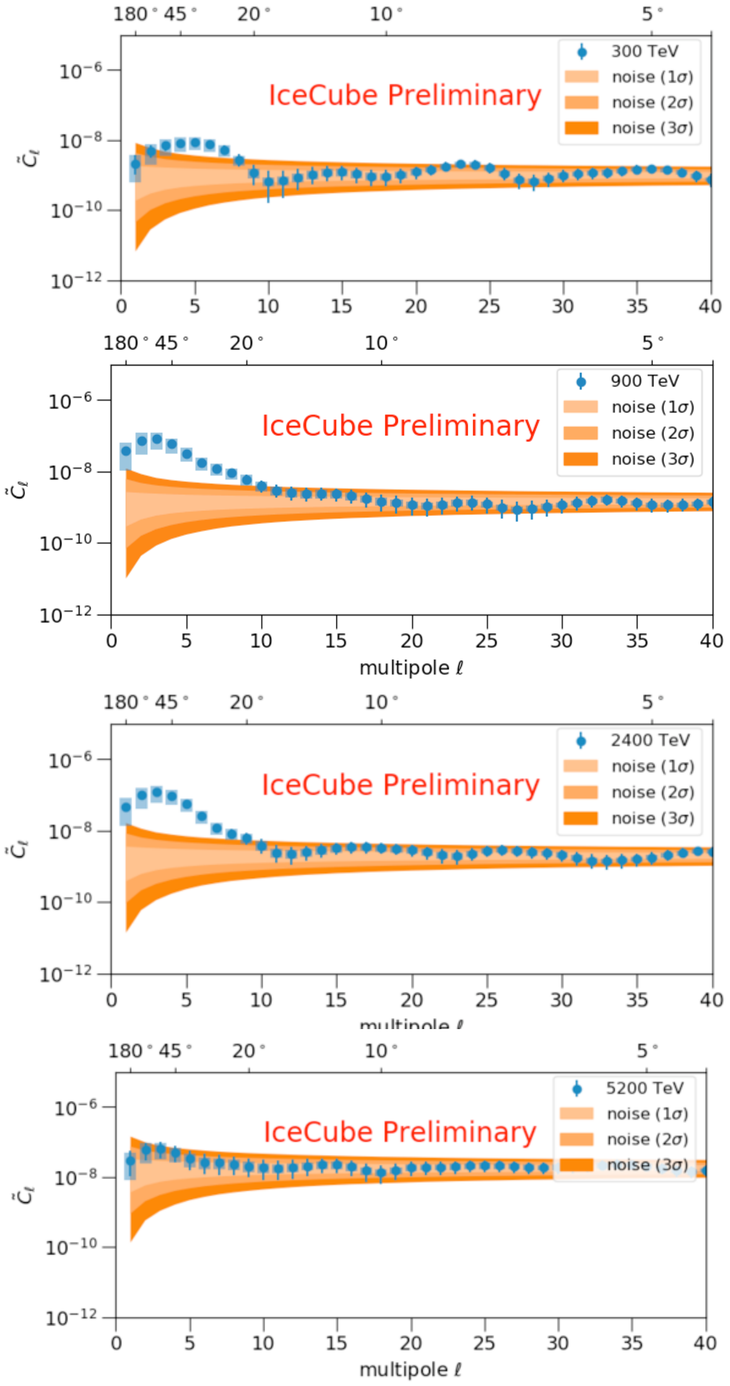
IceTop Anisotropy (TeVPA 2025)





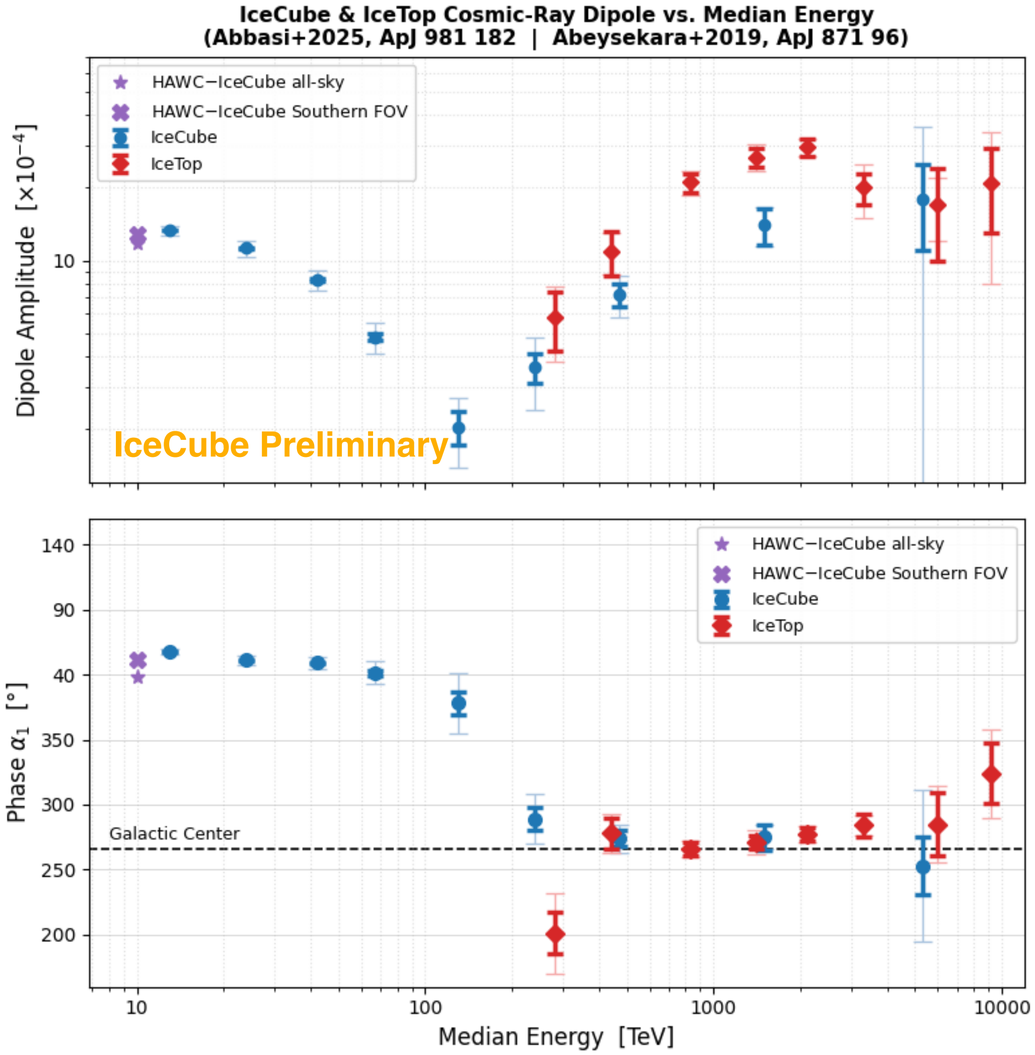






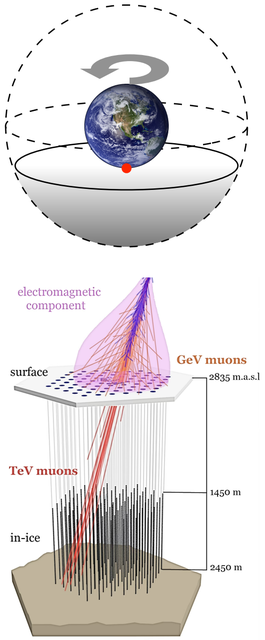
IceCube TeVPA 2025

IceTop/IceCube Rigidity Scaling



IceCube TeVPA 2025

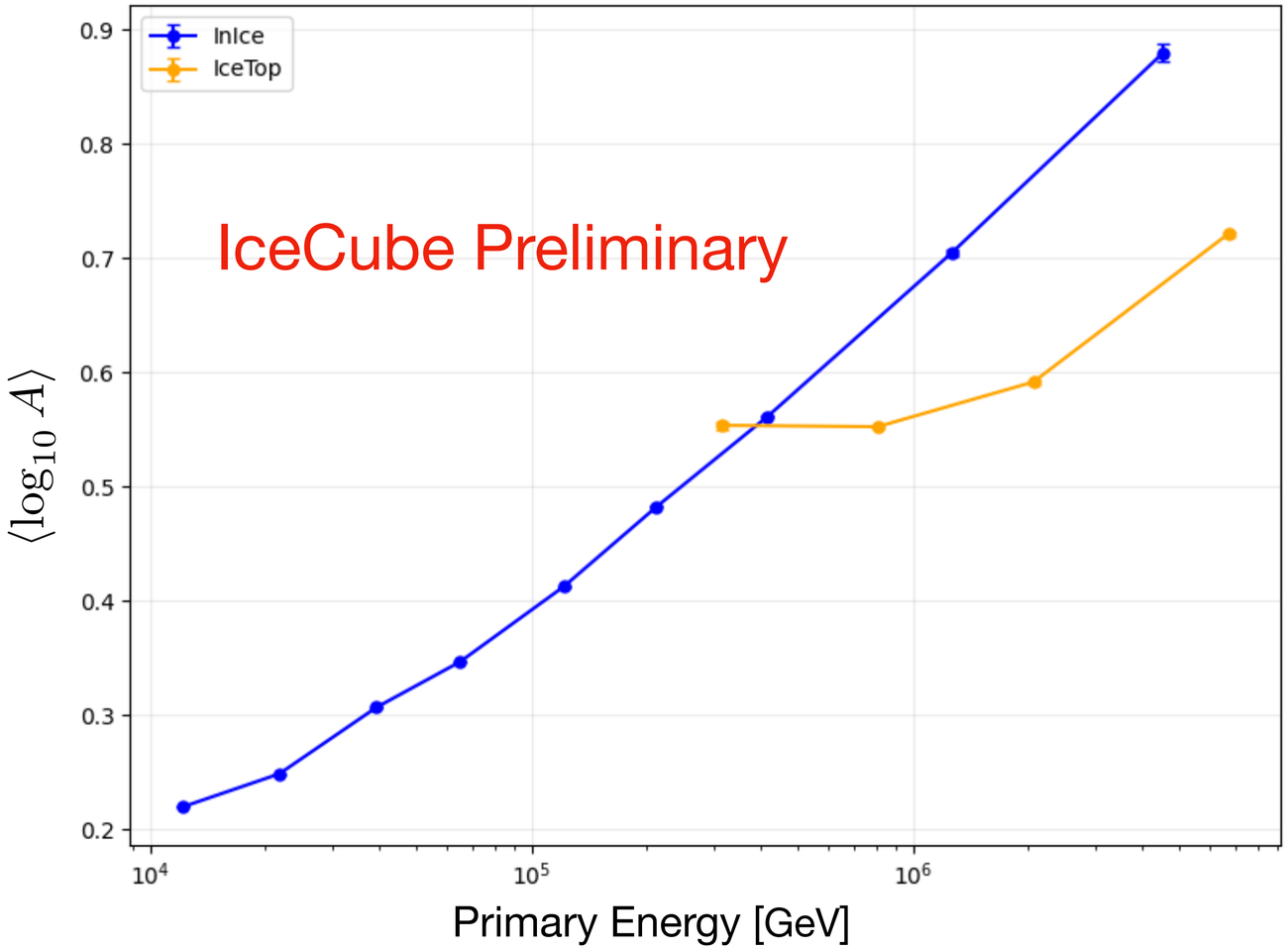
Tension between IceCube and IceTop



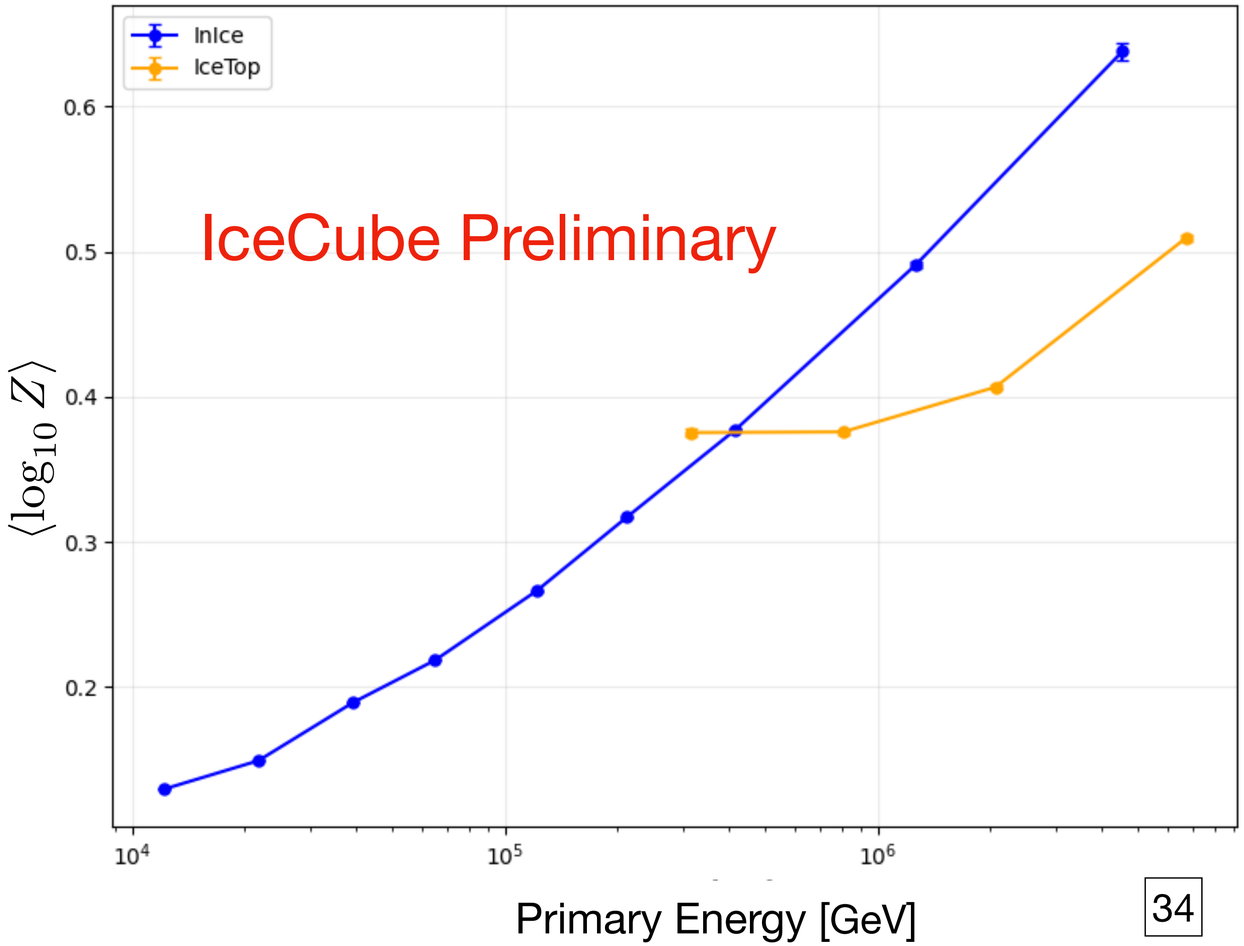
Mass and charge fraction over true energy for InIce and IceTop events.

- Average mass of the primaries in each Set (InIce) or Tier (IceTop).

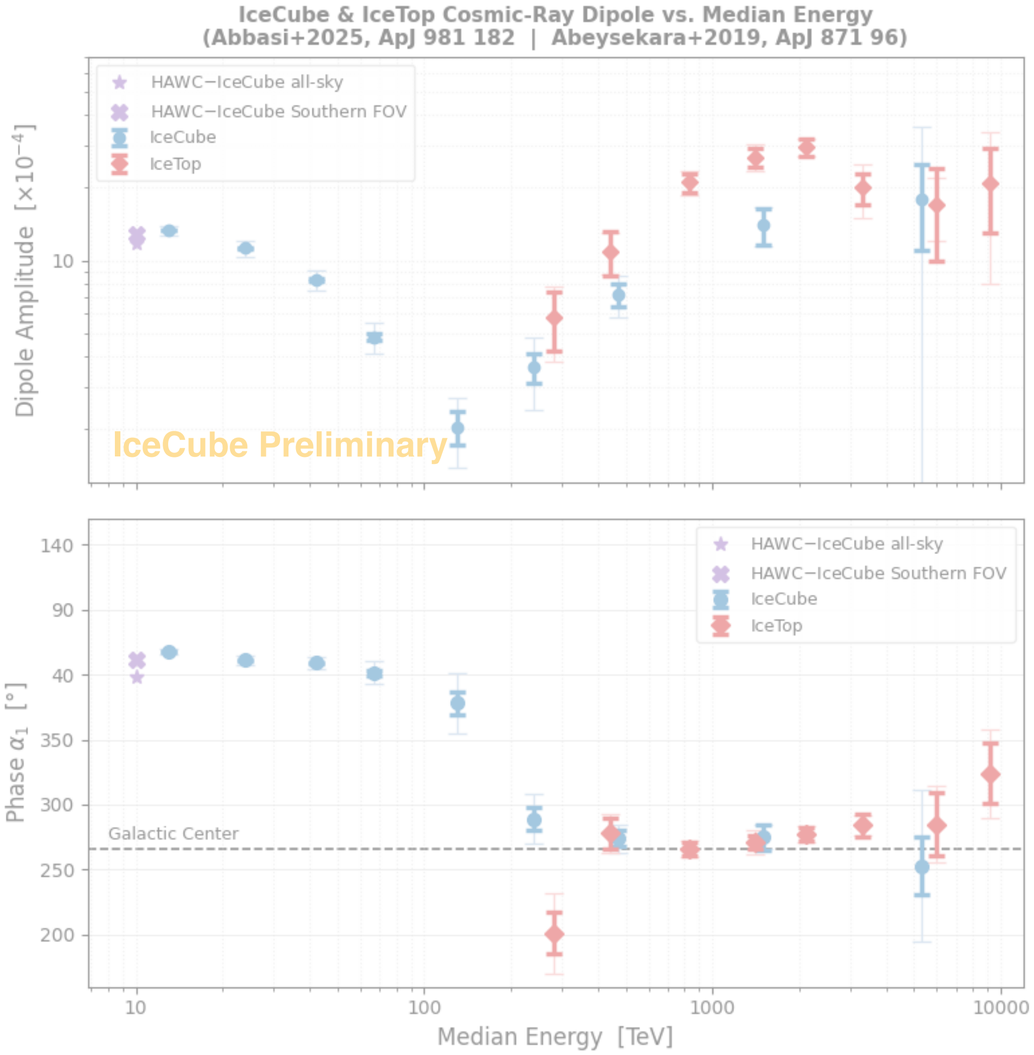
Average mass: $\langle \log_{10}(A) \rangle$

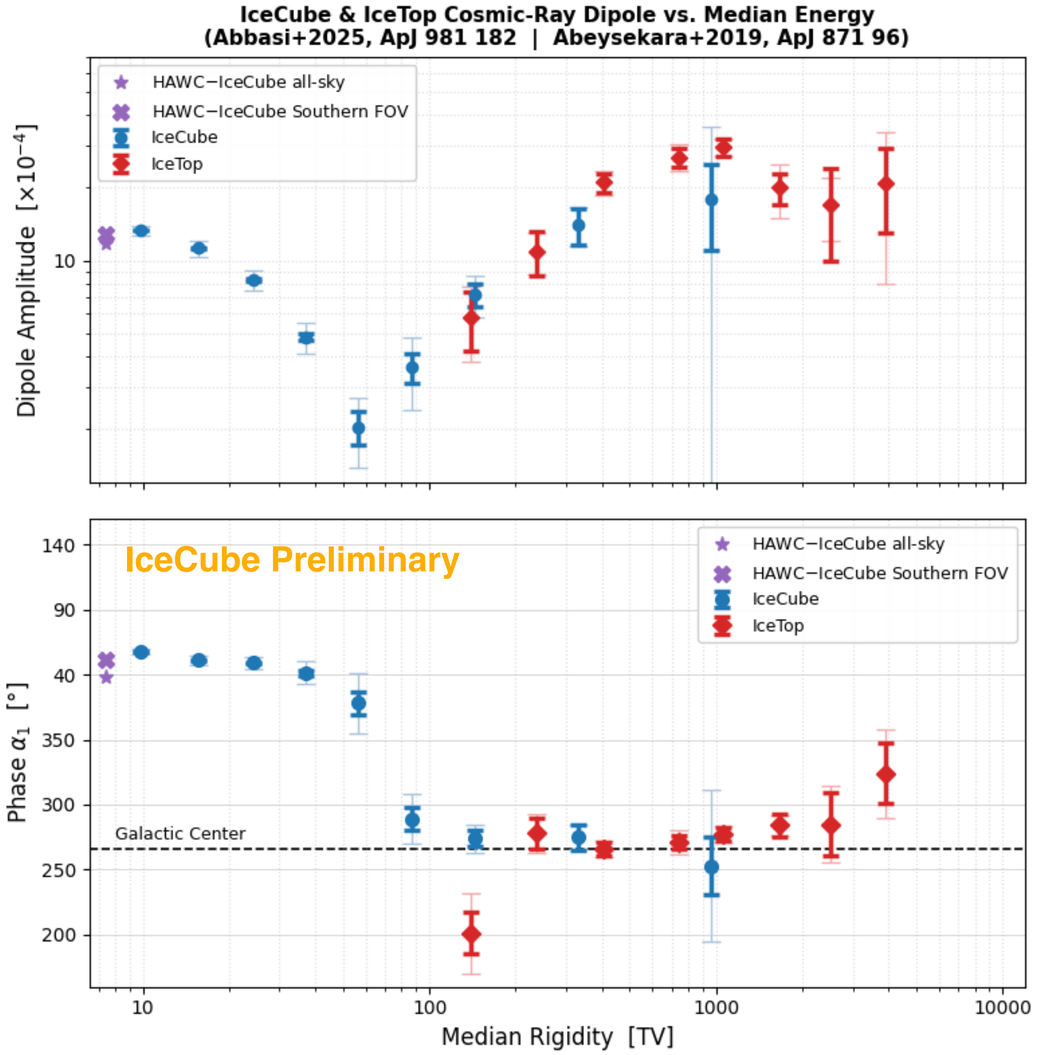


Average charge: $\langle \log_{10}(Z) \rangle$

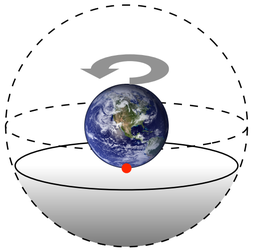


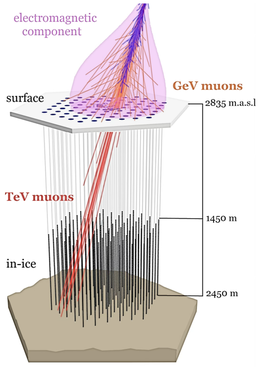
IceTop/IceCube Rigidity Scaling





In rigidity

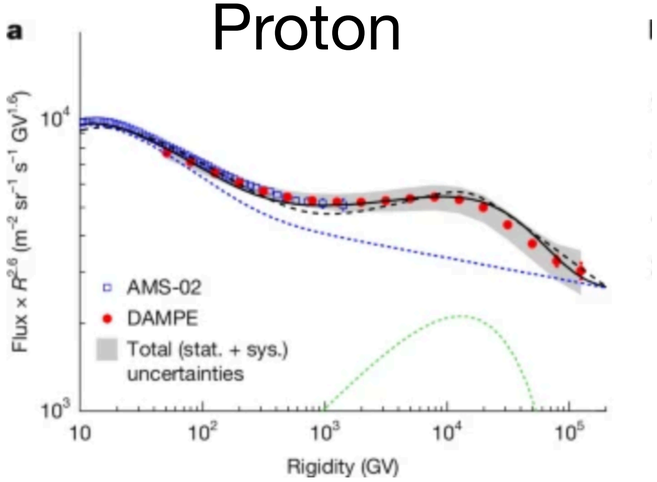


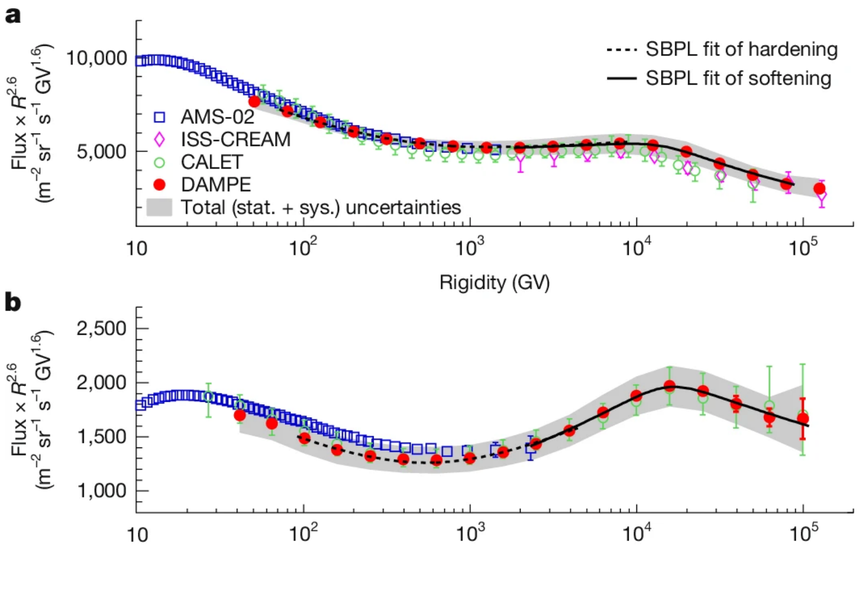


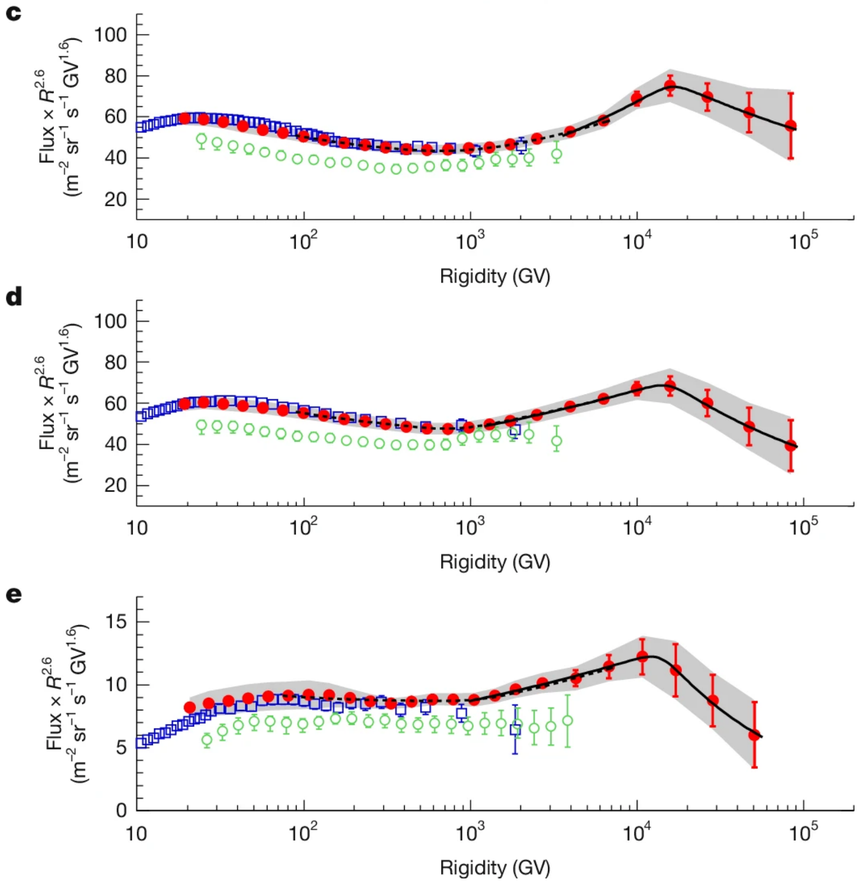
IceCube TeVPA 2025

DAMPE: Charge-dependent spectral softenings of primary cosmic rays below the knee

(**a**), helium (**b**), carbon (**c**), oxygen (**d**) and iron (**e**)

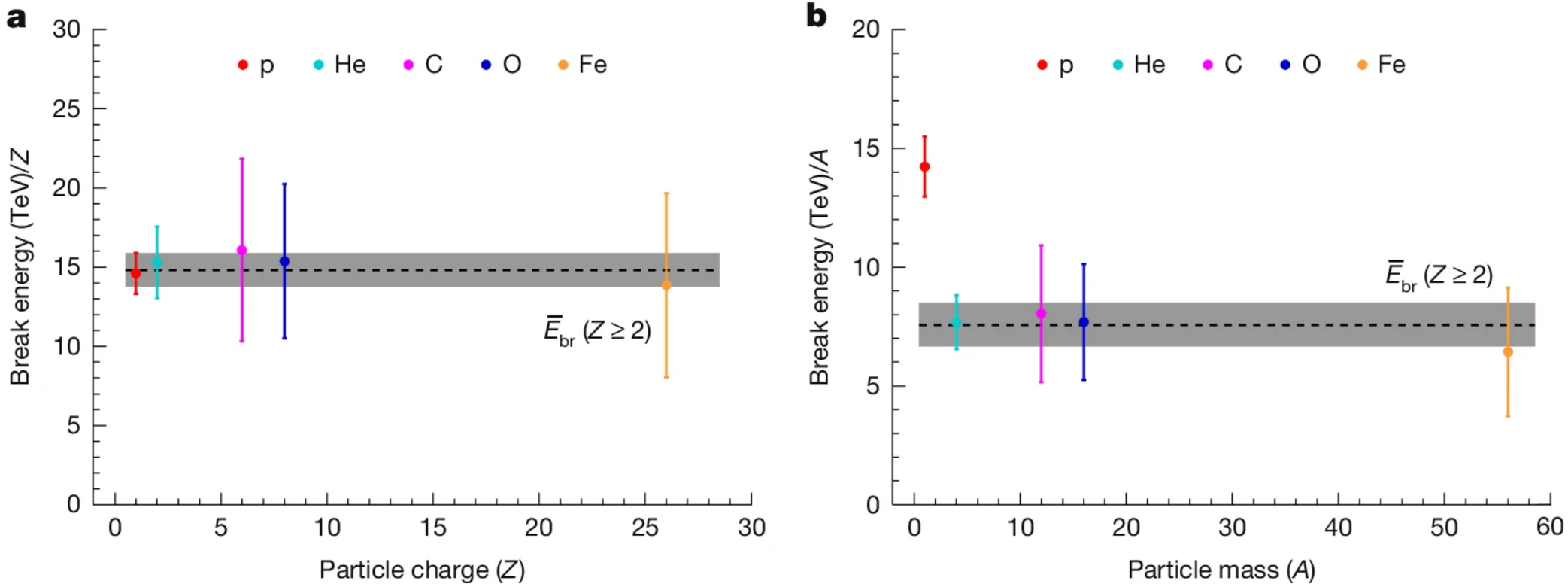






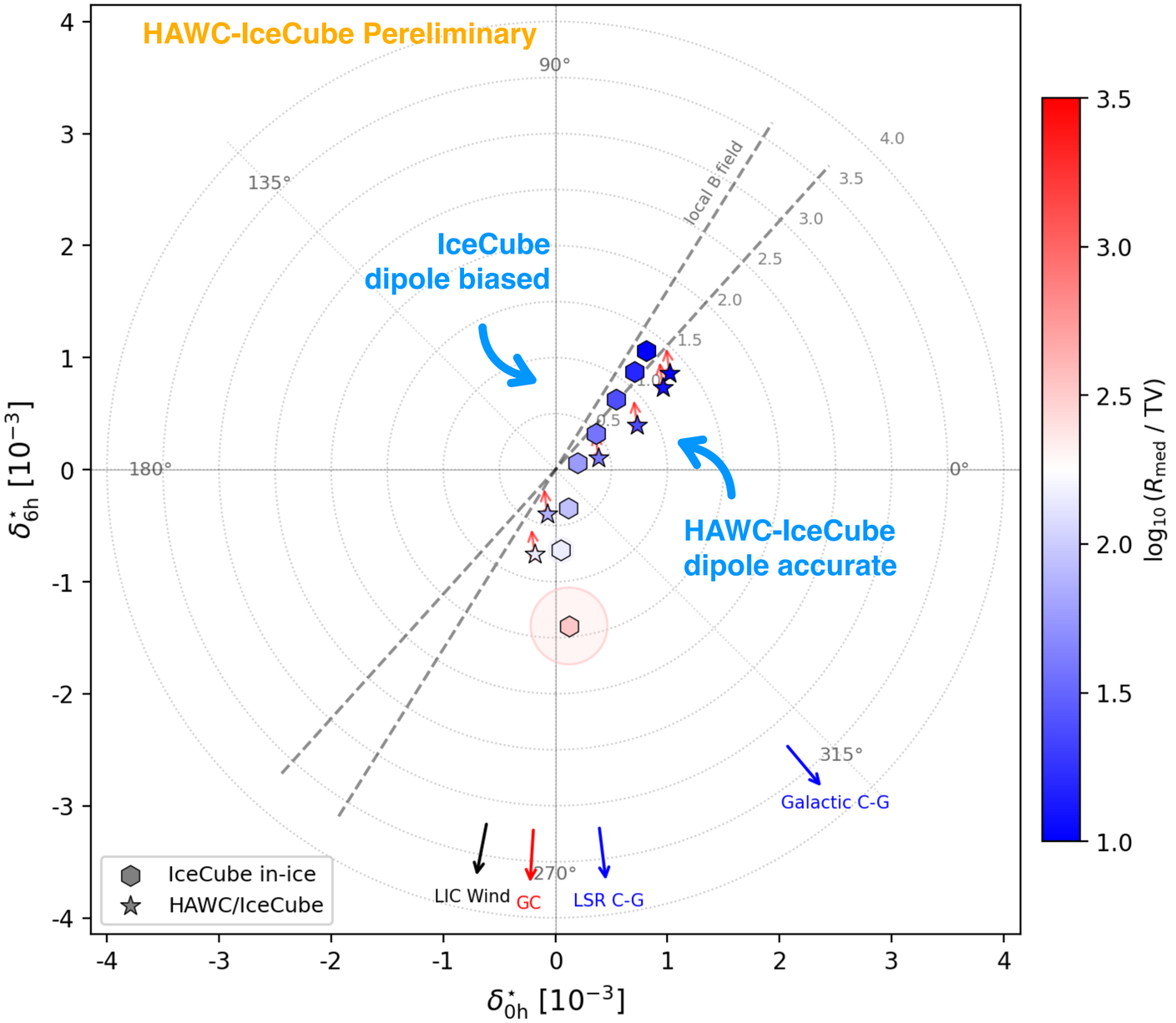
The DAMPE Collaboration
Nature **volume 653**, pages 52–55 (2026)
https://doi.org/10.1038/s41586-026-10472-0

DAMPE: Charge-dependent spectral softenings of primary cosmic rays below the knee



The DAMPE Collaboration
Nature **volume 653**, pages 52–55 (2026)
https://doi.org/10.1038/s41586-026-10472-0

Full-sky vs. partial sky



Expecting alignment to the local ISM magnetic field in the TeV range?

Evidence of Compton-Getting Effect in the Local Standard or Rest?

Propagation transition at 100 TeV?

Is the dipole the relevant diagnostic?

Conclusions

- Observed anisotropy evolves with energy.
  - Generally pointing along LIMF and switching towards GC.
  - Phase flip in the same energy range as break in energy spectrum.
  - Consistent with change in dominant source(s) of CRs.
- Full-sky measurements needed at energies ≥ 1 PeV (IceTop+KASKADE, LHAASO, TALE)
  - Partial sky bias measurements and interpretation of angular power spectrum and spherical harmonics.
  - More observations in the southern hemisphere (SWGO, AMIGA)
  - More collaborations (all of the above)
- Need take CR composition into consideration
  - Strong indication that anisotropy is rigidity dependent rather than energy dependent.
- Bridge the energy gap between 10^{15}–10^{21} eV (AMIGA)

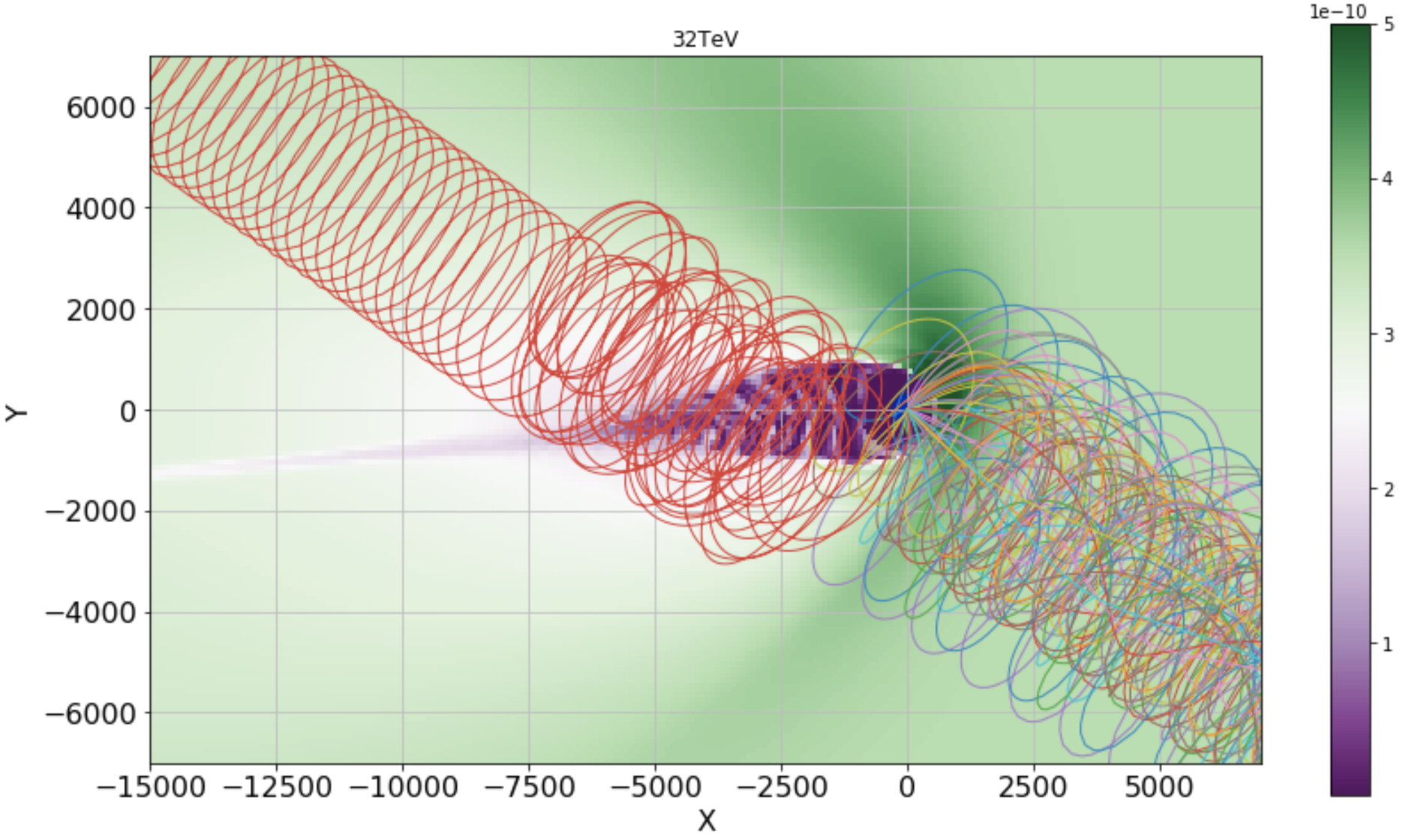
Thank you


Gwenael Gracini
Karen Salomé Caballero Mora
Pravata Mohanty
Ibrahim torres
Pedro Isaac Ramírez Bacá
Elena Orlando
UDEM
INSPIRAN
TU MEJO
VERSIÓN

Backup

TeV Cosmic Rays in the Heliosphere

At higher energies, the heliosphere cannot efficiently trap CR particle anymore



J. C. Díaz-Velez, P. Desiati

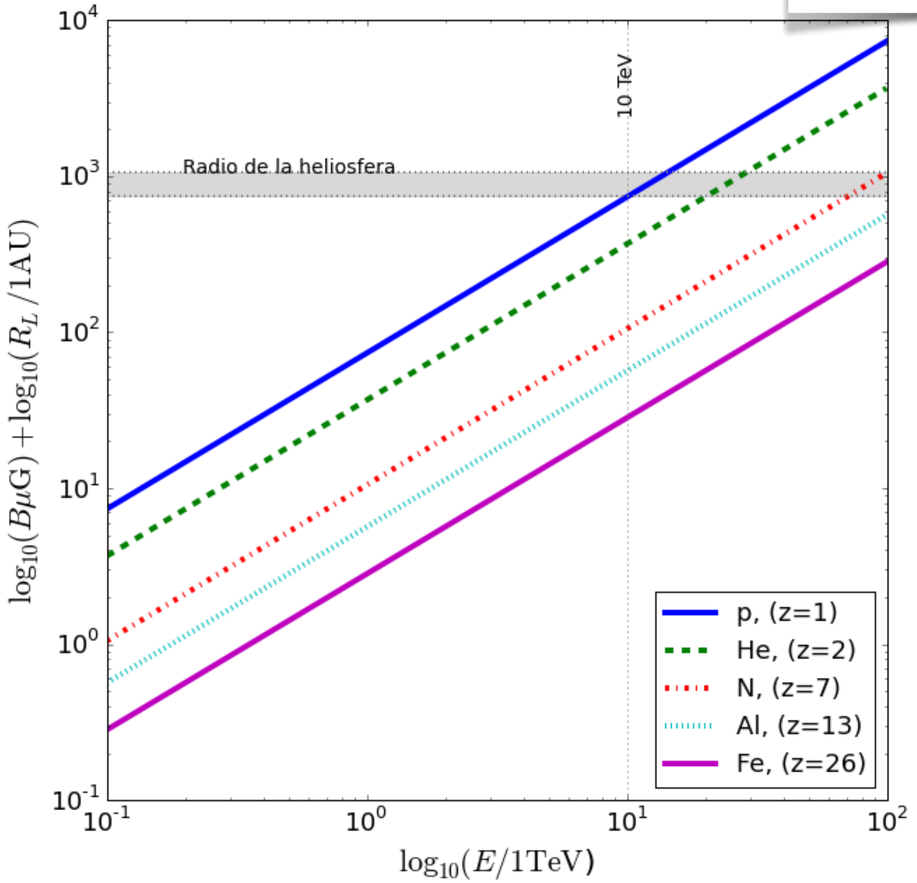
Heliospheric model: Pogorelov et al.(2015)

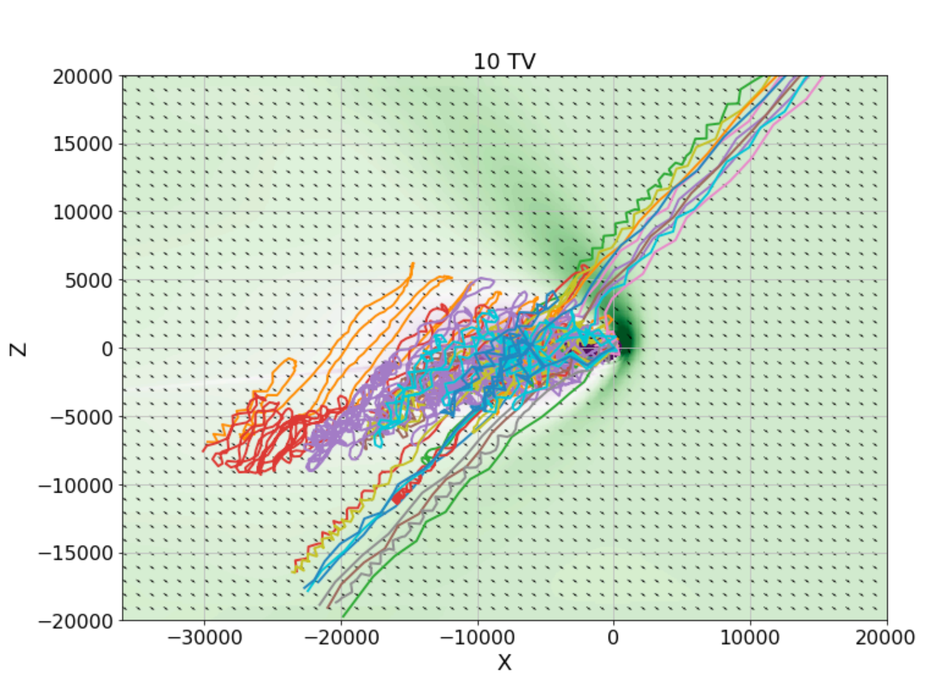
Gyroradius vs Energy

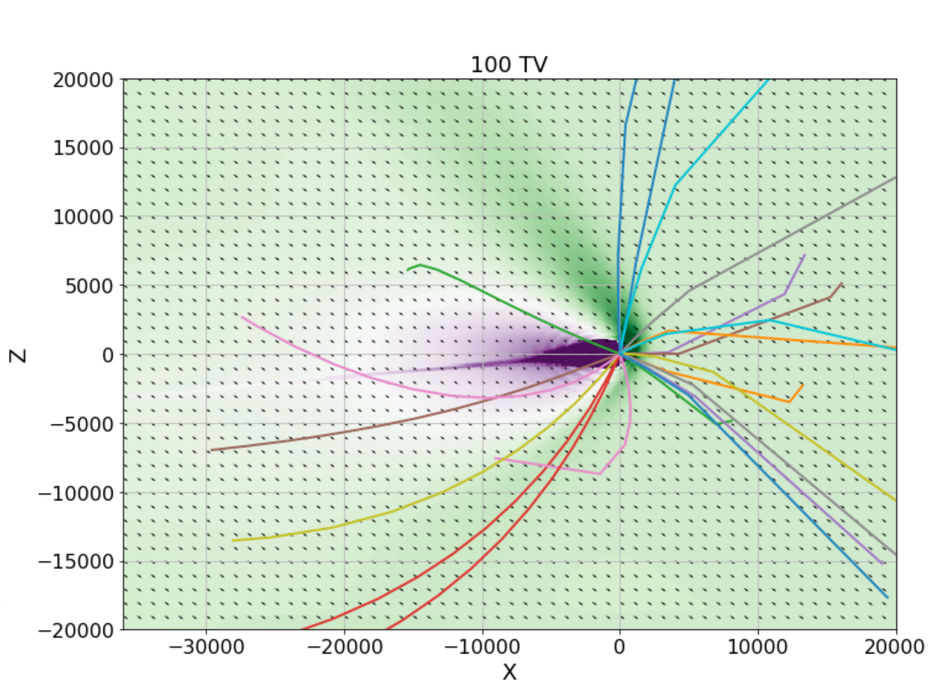
Taking B ~ 3μG (interstellar B-field)

- 1 TeV (proton): R_L ~ 70 UA
- 10 TeV (proton): R_L ~ 700 UA
- 100 TeV (Fe): R_L ~ 282 UA

$$R_L \simeq \frac{220}{z}\left(\frac{E}{1\mathrm{TeV}}\right)\left(\frac{1\mu\mathrm{G}}{B}\right)[\mathrm{AU}]$$







J. C. Díaz-Velez, P. Desiati

Heliospheric model: Pogorelov et al.(2015)

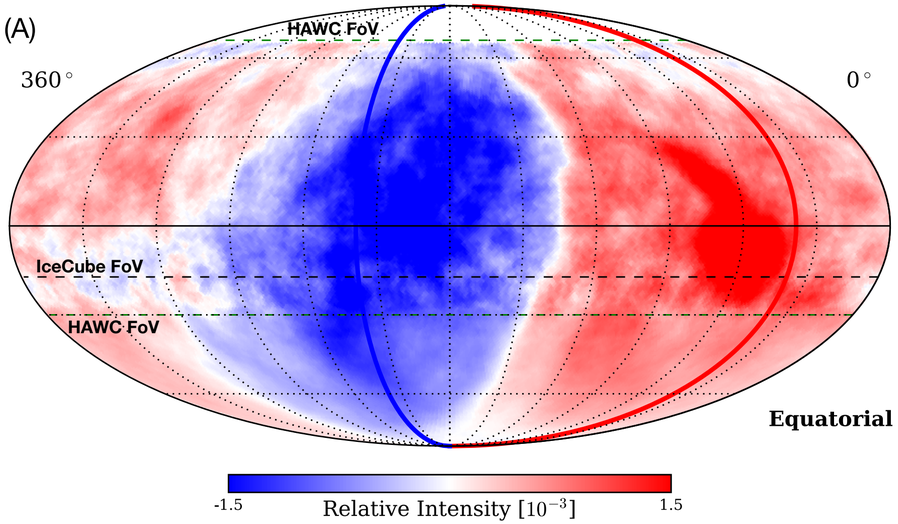
The Astrophysical Journal, 871:96 (15pp), 2019 January 20
https://doi.org/10.3847/1538-4357/aaf5cc
© 2019. The American Astronomical Society. All rights reserved.

CrossMark

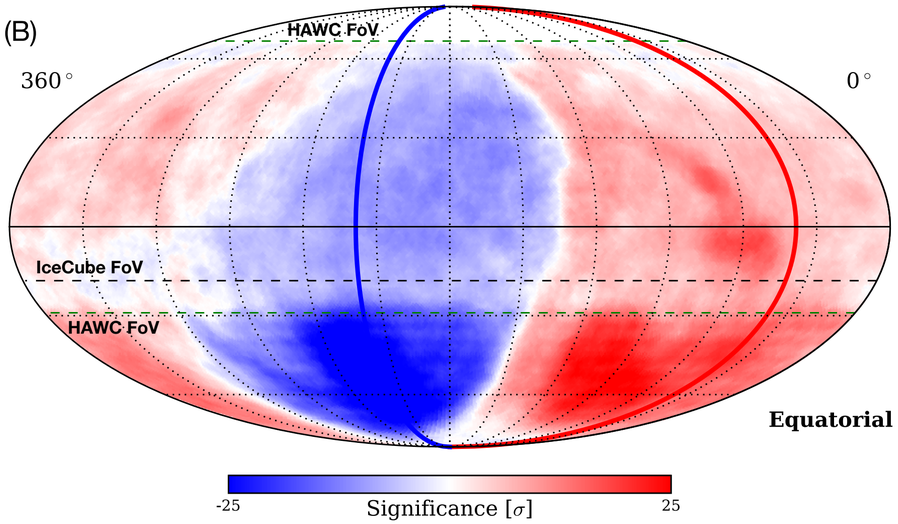
All-sky Measurement of the Anisotropy of Cosmic Rays at 10 TeV and Mapping of the Local Interstellar Magnetic Field

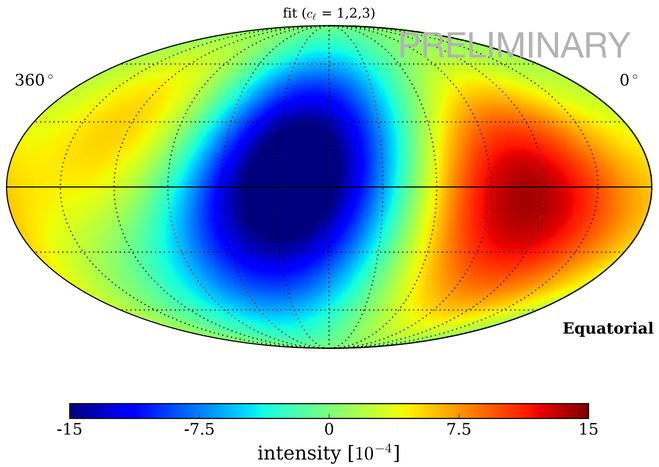
A. U. Abeysekara[1], R. Alfaro[2], C. Alvarez[3], R. Arceo[3], J. C. Arteaga-Velázquez[4], D. Avila Rojas[2], E. Belmont-Moreno[2],

Relative Intensity



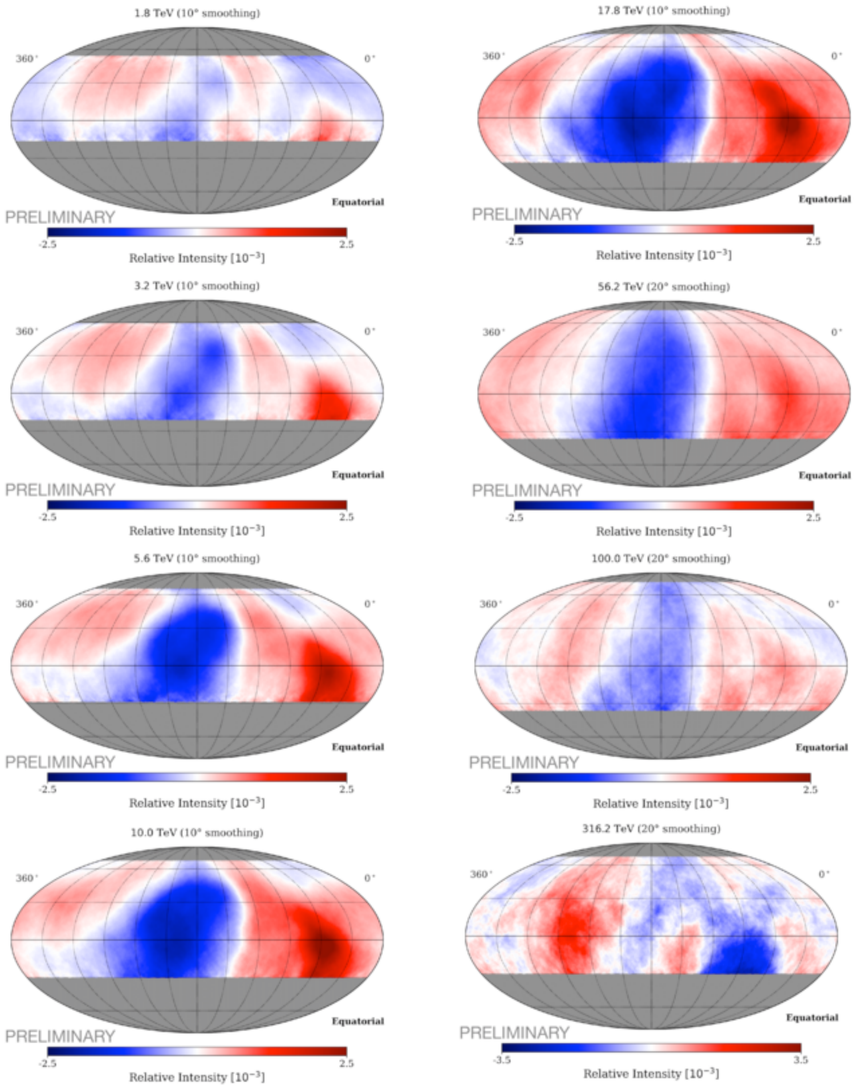
Significance Map





Large Scale

DOI 10.3847/1538-4357/aaf5cc


1.8 TeV (10° smoothing)
360°
0°
Equatorial
PRELIMINARY
-2.5
2.5
Relative Intensity [10^{-3}]
17.8 TeV (10° smoothing)
360°
0°
Equatorial
PRELIMINARY
-2.5
2.5
Relative Intensity [10^{-3}]
3.2 TeV (10° smoothing)
360°
0°
Equatorial
PRELIMINARY
-2.5
2.5
Relative Intensity [10^{-3}]
56.2 TeV (20° smoothing)
360°
0°
Equatorial
PRELIMINARY
-2.5
2.5
Relative Intensity [10^{-3}]
5.6 TeV (10° smoothing)
360°
0°
Equatorial
PRELIMINARY
-2.5
2.5
Relative Intensity [10^{-3}]
100.0 TeV (20° smoothing)
360°
0°
Equatorial
PRELIMINARY
-2.5
2.5
Relative Intensity [10^{-3}]
10.0 TeV (10° smoothing)
360°
0°
Equatorial
PRELIMINARY
-2.5
2.5
Relative Intensity [10^{-3}]
316.2 TeV (20° smoothing)
360°
0°
Equatorial
PRELIMINARY
-3.5
3.5
Relative Intensity [10^{-3}]